Ship Science Report No. 141
ISSN0140-3818

Vibration Problem of a Spherical Tank Containing Jet Propellant: Numerical Simulations

By J. T. Xing, Y. P. Xiong, M. Tan

School of Engineering Sciences, Ship Science,
University of Southampton, Southampton SO171BJ
England

&

Makoto Toyota

Structure & Strength Dept., Research Laboratory, IHI, Japan

December 6, 2006

CONTENTS

Abstract

This document is the final report on the joint research project on vibration problem of a spherical tank containing jet propellant between IHI, Japan and SES, University of Southampton, UK. The background of the project is described. The fundamental principles and numerical method used in numerical simulations are presented. The detailed FEA models for each studied cases are given. The calculation results are presented using tables, curves, figures as well as the attached data files. The available experiment results are listed to compare with the numerical calculations. The calculation results show a fundamental agreement with the experiment results. The numerical analysis confirms that:

1) Due to water – tank interaction, the natural frequencies of the water – tank system are decreased with the water level increase. For the 25% water level, the natural frequencies, especially heave mode frequency, shows a significant decrease compared with the empty case. However, with continuing increase the filed water more than 25% level, the decrease gradient of the natural frequencies gradually tends to zero. In the 100% water case, the natural frequency of heave mode is about 200 Hz which can not equal zero.
2) Considering free surface wave effect produces a lot of sloshing modes of very low frequencies compared with the natural frequencies of the dry tank structure. Therefore, for dynamic response analysis with high frequency excitations, the free surface wave may be neglected. However, to assess loads caused by sloshing modes, the free surface waves have to be considered.
3) There exist relative big deformations at the four tank support places in several vibration modes, which may produce a large local stress at support places to cause the product fail in vibration environment. A strengthen local design at the support places is needed.
4) The dynamic response results are affected by damping coefficients of all modes used in the dynamic response analysis. The damping coefficients are approximately presented and therefore, the numerical results are good reference for practical designs.

The report confirms that the original purpose of this joint research project has well completed by IHI and SES.

Chapter 1 Introduction

1-1 Background

IHI Japan intends to test and analysis the dynamic behaviors of a spherical tank - water interaction system to solve an industry problem.

Professor J T Xing and his colleague in the School of Engineering Sciences (SES) at the University of Southampton (UoS) has produced publications involving theoretical analysis and numerical simulations and has developed software on linear fluid-structure interaction problems in engineering. This background establishes the basis of this joint research between IHI and SES of UoS.

1-2 Objectives

The current joint project research intends to investigate the dynamic behavior of a spherical shell-water interaction system using the experiment and numerical simulations based on linear theory of fluid-structure interaction.

The Project constitutes a part of the following entire study.

1) **Experiment**

   Exciter test of a spherical tank model is performed to measure its natural frequencies and dynamic responses by IHI.

2) **Numerical Simulation** of the experimental tank to obtain its natural frequencies and dynamic responses listed as follows using the computer program developed by SES. The planned calculation cases are:

   a) Empty tank : Natural frequencies and modes,
   One Dynamic response of the tank subjected to a vertical sinusoidal exciter table motion of the frequency (hereinafter referred to as “frequency”) near to the 1-st natural frequency of empty structure.

   b) 1/2 water with no free surface (Eigenvalue, one Dynamic response of frequency near to the fundamental frequency of this whole fluid-structure interaction system).

   c) 1/2 water with free surface (Eigenvalue, one Dynamic response of frequency near to the 1st sloshing frequency of this whole fluid-structure interaction system).

   d) 2/3 water with no free surface (Eigenvalue, one Dynamic response of frequency near to the fundamental frequency of this whole fluid-structure interaction system

e) Fully filled (Eigenvalue, one Dynamic response of frequency near to the fundamental frequency of this whole fluid-structure interaction system)

3) Validation of the calculation results

a) To clarify the phenomenon observed by IHI calculation using its software. That is, with the water volume increasing, the frequency of the water-spherical tank interaction was too low to be physically understood.

b) To compare the calculation frequencies with the experimental results from engineering point.

Dynamic responses are affected by damping, which relies on experiment by IHI and has important effects on the results, especially near to the resonance frequency. Therefore, the responses calculated are a reference for application.

Notes: During the calculation period, the representative of IHI, Mr Makoto Toyoda visited SES, UoS for three months to discuss and modify the previous working plans to provide more practical useful results. After the discussions, it has made the following modifications:

i) Due to the water-shell interactions, the order of vibration modes are changed for different cases, therefore the motion form of the first natural frequency of each case may be different. We determine to choose the frequency of the Heavy mode of shell structure to conduct the dynamic response calculations of the system with no free surface wave consideration.

ii) The first 5 natural frequencies and the corresponding modes are required to be provided in the report.

iii) For the dynamic response analysis of each case, the dynamic response curves at different points are similar so that it is not necessary to draw all response curves at all mea rued points. We determine only to draw the response curves in the vertical direction at the top and bottom points on the shell as well as the pressure curves at the pressure measure points in the report. The all response data for all planed points is provided in the files.

1-3 Description of the Tank

A short description on the tank and exciter system provided by IHI is re-presented herein to make a full document of the report. Fig. 1.1 shows the picture of the model tank. Fig. 1.2 gives the exciter system used in the test. Fig. 1.3 presents a global view of the tank mounted on the vibration table. Fig. 1.4 shows the support part of the tank on the vibration table. The geometrical and physical constants of the tank and water are as follows.

Geometrical and physical constants of the tank

Inner diameter	294.4 mm = 29.44cm
Thickness	2.8mm=0.28cm
Young's modulus	3100MPa = 3.16×10^{4} kg/cm^{2}
Poisson's ratio	0.31
Specific gravity	1190kg/m^{3} $=1.19\times10^{-3}$ kg/cm^{3}

Physical constants of water

Specific gravity	1000kg/m^{3} $=1.0\times10^{-3}$ kg/cm^{3}
Speed of sound	1430m/s

Fig. 1.1 Model tank

Fig. 1.2 Exciter system

Fig. 1.3 A global view of the tank mounted on the vibration table.

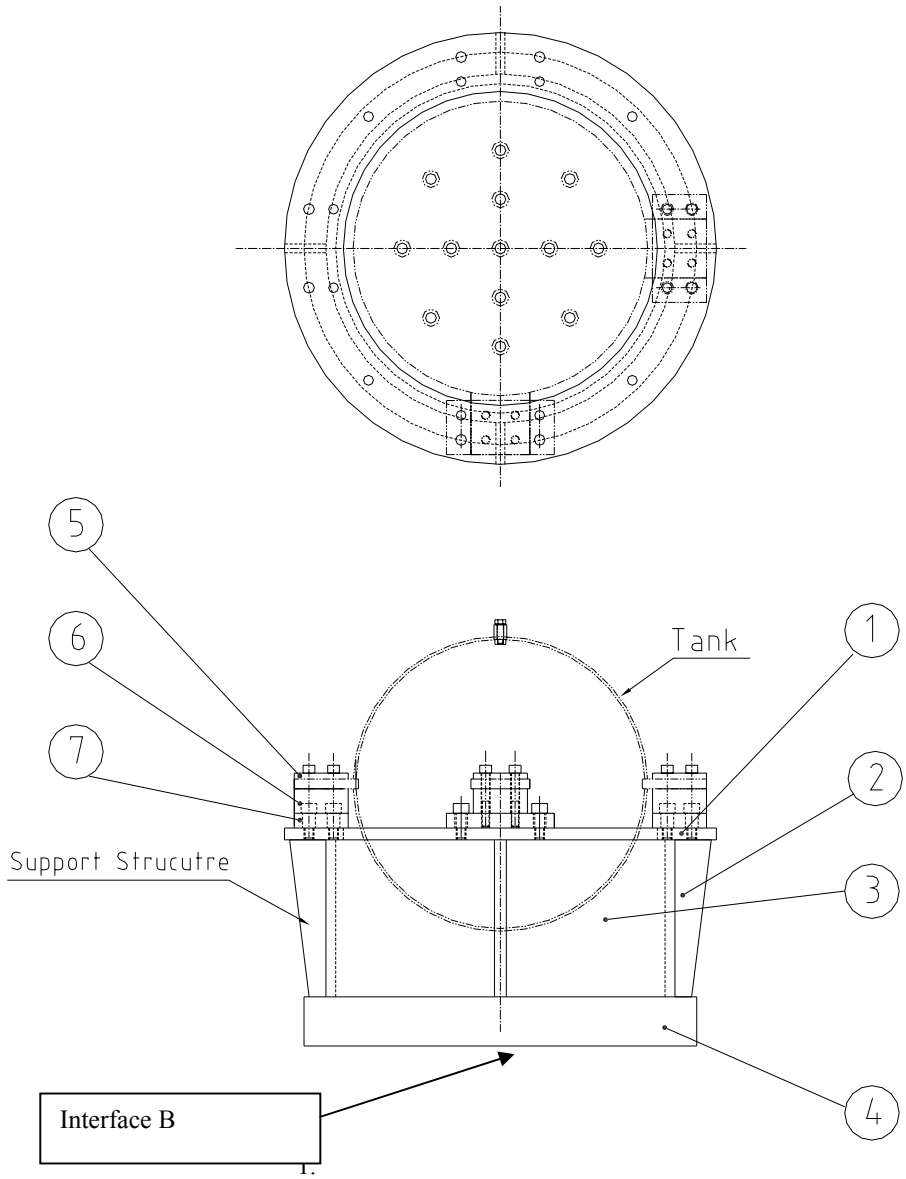

1.
2. Flange
3. Rib
4. Cylinder
5. Base
6. Cover Plate
7. Spacer Block
8. Support Plate

Fig 1.4. Overall view of tank-support structure: Parts 1-4 are welded construction; Parts 5-7 are used to bolt the tank to the support 1-7 are all made of steel Interface B is connected to interface A in Picture 1-2

Positions of sensor points and corresponding node numbers in simulations

Fig. 1.5 shows the positions of measurement points in the test. The corresponding node numbers for each case are listed in Table 1.1-1.5.

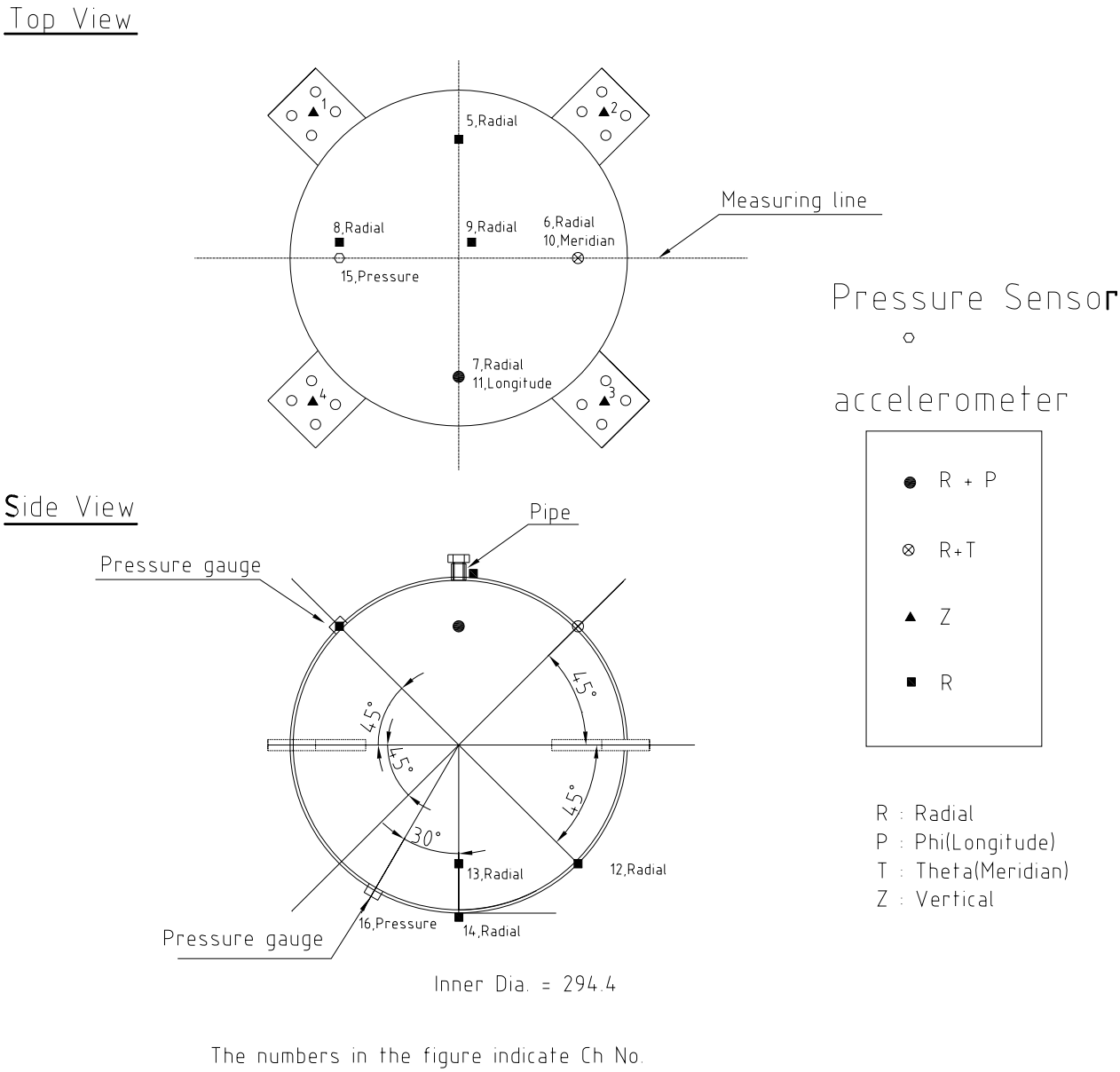

Fig. 1.5 The positions of measurement points in the experiment.

Tables of the node numbers of accelerometer / pressure sensor locations in numerical meshes

There is no node located at the position of pressure sensor 16. Therefore, two points 16a and 16b marked by * are used to give the dynamic response data.

Table 1.1 Empty tank

Sensor number	x	y	z	Node number In FEA
9	0.0000	0.0000	14.8600	836
5	-7.4300	7.4300	10.5076	671
6,10	7.4300	7.4300	10.5076	681
7,11	7.4300	-7.4300	10.5076	652
8	-7.4300	-7.4300	10.5076	642
12	7.4300	7.4300	-10.5076	321
13	7.4300	-7.4300	-10.5076	292
14	0.0000	0.0000	-14.8600	61

Table 1.2 50% water (with and without free surface wave)

Sensor Numbers	x	y	z	Node numbers for 50% water		
				Tank Sub1	WaterSub2	Global
9	0.0000	0.0000	14.8600	836		1646
5	-7.4300	7.4300	+10.5076	671		1481
6,10	7.4300	7.4300	+10.5076	681		1491
7,11	7.4300	-7.4300	+10.5076	652		1462
8	-7.4300	-7.4300	+10.5076	642		1452
12	7.4300	7.4300	-10.5076	321	1131	1131
13	7.4300	-7.4300	-10.5076	292	1102	1102
14	0.0000	0.0000	-14.8600	61	871	871
16a*	4.7704	-4.7704	-13.2400	212	1022	1022
16b*	6.1762	-6.1762	-12.0220	252	1062	1062

Table 1.3 66.7% water

Sensor Numbers	x	y	z	Node numbers for 66.7% water		
				Tank Sub1	WaterSub2	Global
9	0.0000	0.0000	14.8600	876		
5	-7.4300	7.4300	+10.5076	711		
6,10	7.4300	7.4300	+10.5076	721		
7,11	7.4300	-7.4300	+10.5076	692		
8	-7.4300	-7.4300	+10.5076	682		
12	7.4300	7.4300	-10.5076	321	1293	1293
13	7.4300	-7.4300	-10.5076	292	1264	1264
14	0.0000	0.0000	-14.8600	61	1033	1033
16a*	4.7704	-4.7704	-13.2400	212	1184	1184
16b*	6.1762	-6.1762	-12.0220	252	1224	1224

Table 1.4 100% water

Sensor Numbers	x	y	z	Node numbers for 100% Water		
				Tank Sub1	WaterSub2	Global
9	0.0000	0.0000	14.8600	836	2294	2294
5	-7.4300	7.4300	+10.5076	671	2129	2129
6,10	7.4300	7.4300	+10.5076	681	2139	2139
7,11	7.4300	-7.4300	+10.5076	652	2110	2110
8,15	-7.4300	-7.4300	+10.5076	642	2100	2100
12	7.4300	7.4300	-10.5076	321	1779	1779
13	7.4300	-7.4300	-10.5076	292	1750	1750
14	0.0000	0.0000	-14.8600	61	1519	1519
16a*	4.7704	-4.7704	-13.2400	212	1670	1670
16b*	6.1762	-6.1762	-12.0220	252	1710	1710

Chapter 2 Theoretical Modeling and Numerical Method

In this chapter, a brief description on the general fluid-structure interaction theory and numerical method with the software used in this project is presented. The detailed mathematics and practical examples can be read in the publication papers (Xing and Price 1991, Xing , Price and Du 1996, Xing, Price and Wang 1997).

2-1 Governing Equations of the Fluid-Structure Interaction System

Fig. 2.1 shows a generalized fluid-structure interaction system consisting of a flexible structure of mass density ρ_s within a domain Ω_s of boundary $S_T \cup S_w \cup \Sigma$ with its unit normal vector ν_i and a fluid in a domain Ω_f of boundary $\Gamma_f \cup \Gamma_p \cup \Gamma_w \cup \Sigma$ with a unit normal vector η_i.

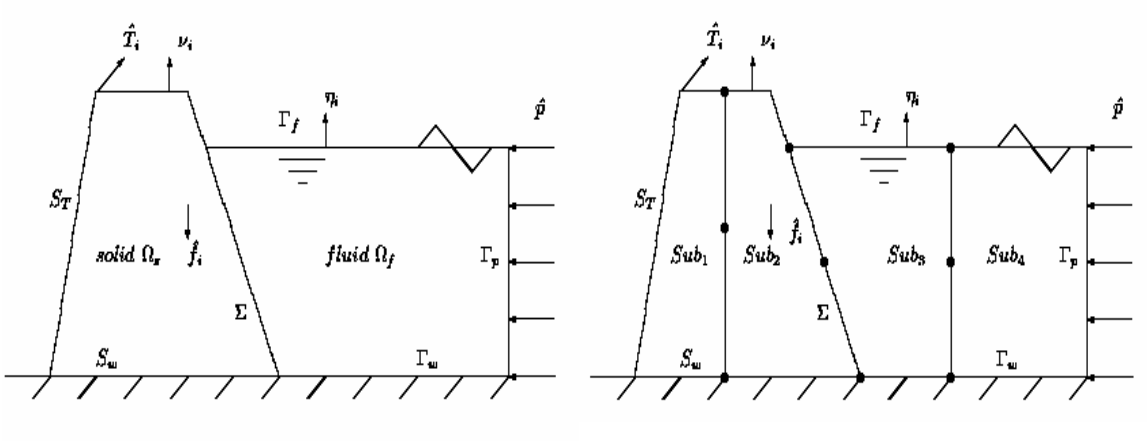

Fig.2.1 Schematic illustration of a general fluid - structure interaction system

The system is excited by external dynamical forces $\hat{T}_i$, $\hat{f}_i$, $\hat{p}$ and ground acceleration $\hat{w}_i$. The Cartesian tensor notations (Fung 1977) with subscripts *i*, *j*, *k* and *l* (=1,2,3) obeying the summation convention are used in the paper. For example, u_i, v_i, w_i, e_{ij}, σ_{ij} and E_{ijkl} represent displacement, velocity, acceleration vector, strain, stress and elastic tensor in the solid, respectively, *p* denotes the pressure in the fluid. The governing equations describing the dynamics of the coupled fluid - structure interaction problems are as follows.

Solid Domain

Dynamic equation

$$\sigma_{ij,j} + \hat{f}_i = \rho_s w_i , \qquad (x_i , t) \in \Omega_s \times (t_1, t_2). \tag{1}$$

Strain-displacement

$$e_{ij} = \frac{1}{2}(u_{i,j} + u_{j,i}), \quad (x_i, t) \in \Omega_s \times (t_1, t_2). \tag{2}$$

Constitutive equation

$$\sigma_{ij} = E_{ijkl} e_{kl}, \qquad (x_i, t) \in \Omega_s \times (t_1, t_2). \tag{3}$$

and, assuming linearity, we have

$$v_i = u_{i,t}, \; w_i = v_{i,t}, \; d_{i,j} = e_{ij,t} = \frac{1}{2}(v_{i,j} + v_{j,i}). \tag{4}$$

Boundary conditions

$$\text{acceleration:} \quad w_i = \hat{w}_i, \quad (x_i, t) \in S_w \times [t_1, t_2], \tag{5-1}$$

$$\text{traction:} \quad \sigma_{ij} \nu_j = \hat{T}_i, \quad (x_i, t) \in S_T \times [t_1, t_2], \tag{5-2}$$

Fluid Subdomain

There are two parts for the fluid domain. One is water and another is air. Here, superscript β is used to distinguish fluid domain number. For illustration purpose, it is assumed that two fluid domains are used and therefore $\beta = 1, \; 2$ in this report.

Dynamic equation

$$p^{(\beta)}_{,tt} = (c^2)^{(\beta)} p^{(\beta)}_{,ii}, \quad (x_i, t) \in \Omega_f^{(\beta)} \times (t_1, t_2). \tag{6}$$

Boundary conditions

free surface:

$$p^{(\beta)}_{,i} \eta_i^{(\beta)} = -p^{(\beta)}_{,tt} / g, \qquad (x_i, t) \in \Gamma_f^{(\beta)} \times [t_1, t_2], \tag{7}$$

pressure:

$$p^{(\beta)} = \hat{p}^{(\beta)}, \qquad (x_i, t) \in \Gamma_p^{(\beta)} \times [t_1, t_2], \tag{8}$$

acceleration:

$$p^{(\beta)}_{,i} \eta_i^{(\beta)} = -\rho_f^{(\beta)} \hat{w}_i^{(\beta)} \eta_i^{(\beta)}, \qquad (x_i, t) \in \Gamma_w^{(\beta)} \times [t_1, t_2]. \tag{9}$$

Interaction interfaces

liquid interface between two fluid domains $\beta = 1, \; 2$:

$$\frac{1}{\rho_f^{(1)}} p_{,i}^{(1)} \eta_i^{(1)} + \frac{1}{\rho_f^{(2)}} p_{,i}^{(2)} \eta_i^{(2)} = 0, \tag{10-1}$$

$$p^{(1)} = p^{(2)}, \qquad (x_i, t) \in \Gamma^{(12)} \times [t_1, t_2], \tag{10-2}$$

where the gravitational potential of the air on the interface is neglected.

Fluid-Structure Interaction Interface:

$$w_i \nu_i = p_{,i}^{(\beta)} \eta_i^{(\beta)} / \rho_f^{(\beta)}, \quad (x_i, t) \in \Sigma^{(\beta)} \times [t_1, t_2], \tag{11-1}$$

$$\sigma_{ij} \nu_j = p^{(\beta)} \eta_i^{(\beta)}, \qquad (x_i, t) \in \Sigma^{(\beta)} \times [t_1, t_2]. \tag{11-2}$$

2-2 Variational Formulations and FE Substructure-Subdomain Method

The variational principle (Xing & Price 1991, 1996) is extended to its substructure – subdomain form as follows:

$$H_{sf}[p, w_i] = H_s[w_i] + H_{f\beta}[p] + H_{\Sigma\beta}[p, w_i], \tag{12-1}$$

$$H_s[w_i] = \int_{t_1}^{t_2} \{ \int_{\Omega_s^{(I)}} (\frac{1}{2} \rho_s w_i \, w_i \, - \frac{1}{2} E_{ijkl} d_{ij} d_{kl} - \hat{f}_i \, w_i \,) d\Omega_s - \int_{S_T^{(I)}} \hat{T}_i \, w_i \, dS \, \} dt \,, \tag{12-2}$$

$$H_{\Sigma\beta}[p, w_i] = -\sum_{\beta} \int_{t_1}^{t_2} \int_{\Sigma^{(\beta)}} p^{(\beta)} w_i^{(\beta)} \eta_i^{(\beta)} d\Gamma^{(\beta)} dt, \tag{12-3}$$

$$\begin{aligned} H_{f\beta}[p] = \sum_{\beta} \int_{t_1}^{t_2} \{ & \int_{\Omega_f^{(\beta)}} \frac{1}{2} [\frac{p_{,t}^{(\beta)} p_{,t}^{(\beta)}}{\rho_f^{(\beta)} c^{2(\beta)}} - \frac{p_{,i}^{(\beta)} p_{,i}^{(\beta)}}{\rho_f^{(\beta)}}] d\Omega_f^{(\beta)} + \int_{\Gamma_f^{(\beta)}} \frac{p_{,t}^{(\beta)} p_{,t}^{(\beta)}}{2 \rho_f^{(\beta)} g} d\Gamma^{(\beta)} \\ & - \int_{\Gamma_w^{(\beta)}} p^{(\beta)} \hat{w}_i^{(\beta)} \eta_i^{(\beta)} d\Gamma^{(\beta)} \} dt \end{aligned} \,. \tag{12-4}$$

This functional is subject to the constraints given in Eqs 2, 4, 5-1,_8 and 10-2 as well as the imposed variation constraints $\delta v_i = 0 = \delta p^{(\beta)}$ at the two time terminals $t_1$and t_2. The stationary conditions of the functional given in Eq.12 are described in Eqs 1, 5-2, 6, 7, 9, 10-1, 11.

A discretization of the solid and fluid media into finite elements expresses the displacement of the solid and the pressure of the fluid using FEA interpolations (Bathe, 1996; Zienkiewicz & Taylor 1989, 1991) in the forms

$$\mathbf{u} = \begin{Bmatrix} u_1 \\ u_2 \\ u_3 \end{Bmatrix} = \mathbf{\Psi U}\,, \tag{13-1}$$

$$p^{(\beta)} = \mathbf{\Theta p}^{(\beta)}\,, \tag{13-2}$$

where $\mathbf{\Psi}$ and $\mathbf{\Theta}^{(\beta)}$ denote the interpolation function matrices and $\mathbf{U}$ and $\mathbf{p}^{(\beta)}$ represent the global node displacement / pressure vector, respectively. The functional H_{sf} given in Eq. 12 now takes the form

$$\begin{aligned} H_{sf}[\mathbf{p}, \ddot{\mathbf{U}}] = \int_{t_1}^{t_2} (\frac{1}{2}\ddot{\mathbf{U}}^T \mathbf{M}\ddot{\mathbf{U}} - \frac{1}{2}\dot{\mathbf{U}}^T \mathbf{K}\ \dot{\mathbf{U}} - \ddot{\mathbf{U}}^T \hat{\mathbf{F}})\ dt - \sum_{\beta}\ \int_{t_1}^{t_2} (\mathbf{p}^T \mathbf{R}\ddot{\mathbf{U}})^{(\beta)}\, dt \\ + \sum_{\beta}\ \int_{t_1}^{t_2} (\frac{1}{2}\dot{\mathbf{p}}^T \mathbf{m}\ \dot{\mathbf{p}}\ - \frac{1}{2}\mathbf{p}^T \mathbf{k}\ \mathbf{p}\ - \mathbf{p}^T \hat{\ddot{\mathbf{u}}})^{(\beta)}\, dt, \end{aligned} \tag{14}$$

where $\mathbf{M}$ and $\mathbf{K}$ represent respectively the finite-element mass and stiffness matrices of the dry structure; $\mathbf{m}^{(\beta)}$ and $\mathbf{k}^{(\beta)}$ represent the finite-element matrices of the fluid domain, $\mathbf{R}^{(\beta)}$ denotes the fluid-structure interaction matrix.

The stationary conditions of the functional in Eq.14 is the finite equation of the air - liquid - structure dynamic interaction system

$$\begin{bmatrix} \mathbf{M} & \mathbf{0} & \mathbf{0} \\ \mathbf{R}^{(1)} & \mathbf{m}^{(1)} & \mathbf{0} \\ \mathbf{R}^{(2)} & \mathbf{0} & \mathbf{m}^{(2)} \end{bmatrix} \begin{Bmatrix} \ddot{\mathbf{U}} \\ \ddot{\mathbf{p}}^{(1)} \\ \ddot{\mathbf{p}}^{(2)} \end{Bmatrix} + \begin{bmatrix} \mathbf{K} & -\mathbf{R}^{(1)\mathrm{T}} & -\mathbf{R}^{(2)\mathrm{T}} \\ \mathbf{0} & \mathbf{k}^{(1)} & \mathbf{0} \\ \mathbf{0} & \mathbf{0} & \mathbf{k}^{(2)} \end{bmatrix} \begin{Bmatrix} \mathbf{U} \\ \mathbf{p}^{(1)} \\ \mathbf{p}^{(2)} \end{Bmatrix} = \begin{Bmatrix} \mathbf{F} \\ \mathbf{f}^{(1)} \\ \mathbf{f}^{(2)} \end{Bmatrix}. \tag{15}$$

Introduce the following matrices

$$\begin{aligned} \mathbf{R} = \begin{Bmatrix} \mathbf{R}^{(1)} \\ \mathbf{R}^{(2)} \end{Bmatrix}, \qquad \mathbf{p} = \begin{Bmatrix} \mathbf{p}^{(1)} \\ \mathbf{p}^{(2)} \end{Bmatrix}, \qquad \mathbf{f} = \begin{Bmatrix} \mathbf{f}^{(1)} \\ \mathbf{f}^{(2)} \end{Bmatrix}, \\ \mathbf{m} = \begin{bmatrix} \mathbf{m}^{(1)} & \mathbf{0} \\ \mathbf{0} & \mathbf{m}^{(2)} \end{bmatrix}, \qquad \mathbf{k} = \begin{bmatrix} \mathbf{k}^{(1)} & \mathbf{0} \\ \mathbf{0} & \mathbf{k}^{(2)} \end{bmatrix}, \end{aligned} \tag{16}$$

then Eq.15 becomes

$$\begin{bmatrix} \mathbf{M} & \mathbf{0} \\ \mathbf{R} & \mathbf{m} \end{bmatrix} \begin{Bmatrix} \ddot{\mathbf{U}} \\ \ddot{\mathbf{p}} \end{Bmatrix} + \begin{bmatrix} \mathbf{K} & -\mathbf{R}^T \\ \mathbf{0} & \mathbf{k} \end{bmatrix} \begin{Bmatrix} \mathbf{U} \\ \mathbf{p} \end{Bmatrix} = \begin{Bmatrix} \mathbf{F} \\ \mathbf{f} \end{Bmatrix}, \tag{17}$$

which can be transformed into the symmetric form (Xing & Price, 1991) as

$$\begin{bmatrix} \mathbf{M} & \mathbf{0} \\ \mathbf{0} & \mathbf{m} \end{bmatrix} \begin{Bmatrix} \ddot{\mathbf{U}} \\ \ddot{\mathbf{p}} \end{Bmatrix} + \begin{bmatrix} \mathbf{K}^T\mathbf{M}^{-1}\mathbf{K} & -\mathbf{K}^T\mathbf{M}^{-1}\mathbf{R}^T \\ -\mathbf{R}\mathbf{M}^{-1}\mathbf{K} & \mathbf{k}+\mathbf{R}^T\mathbf{M}^{-1}\mathbf{R}^T \end{bmatrix} \begin{Bmatrix} \mathbf{U} \\ \mathbf{p} \end{Bmatrix} = \begin{Bmatrix} \mathbf{F} \\ \mathbf{f} \end{Bmatrix}, \tag{18}$$

This equation can be solved by using a mode superposition method or a time integral method as usually adopted in a general finite element analysis. For natural vibrations of the system, the force vector on the right hand side of Eq.18 vanishes.

2-3 Brief introductions on software FSIAP

To complement the mixed finite element substructure-subdomain method presented herein, a specialized *Fluid – Structure Interaction Analysis Program-FSIAP* (Xing 1995a, b) based on PC computer architecture was further developed to solve natural vibration and dynamical response problems associated with structure, fluids and their interactions. This user-friendly software contains all the theoretical features discussed in the development of the approach and overcomes restrictions on computer storage capacity, length of run time etc, providing an efficient solution to complex fluid-structure dynamical interaction problems. The main flow chart of FSIAP is shown in Fig.2.2 Here, this program is used to calculate the natural characteristics and dynamic responses excited by base motion of the water tank interaction system.

The engineering unit system is used in the program. That is

Length	cm
Force	kg
Time	s

The output data can give the natural frequencies and the corresponding natural modes as well as the dynamic responses of the system excited forces applied or the ground motion. The dynamic response output data is given in the following format.

*** Node number * - (Component number)** defined as:

Node number: node number in the substructure or subdomain mesh,

Component number = 1 x- direction displacement

= 2 y- direction displacement

= 3 z- direction displacement

= 4 rotation about x- direction

= 5 rotation about y- direction

= 6 rotation about z- direction

= 7 fluid pressure in fluid subdomain

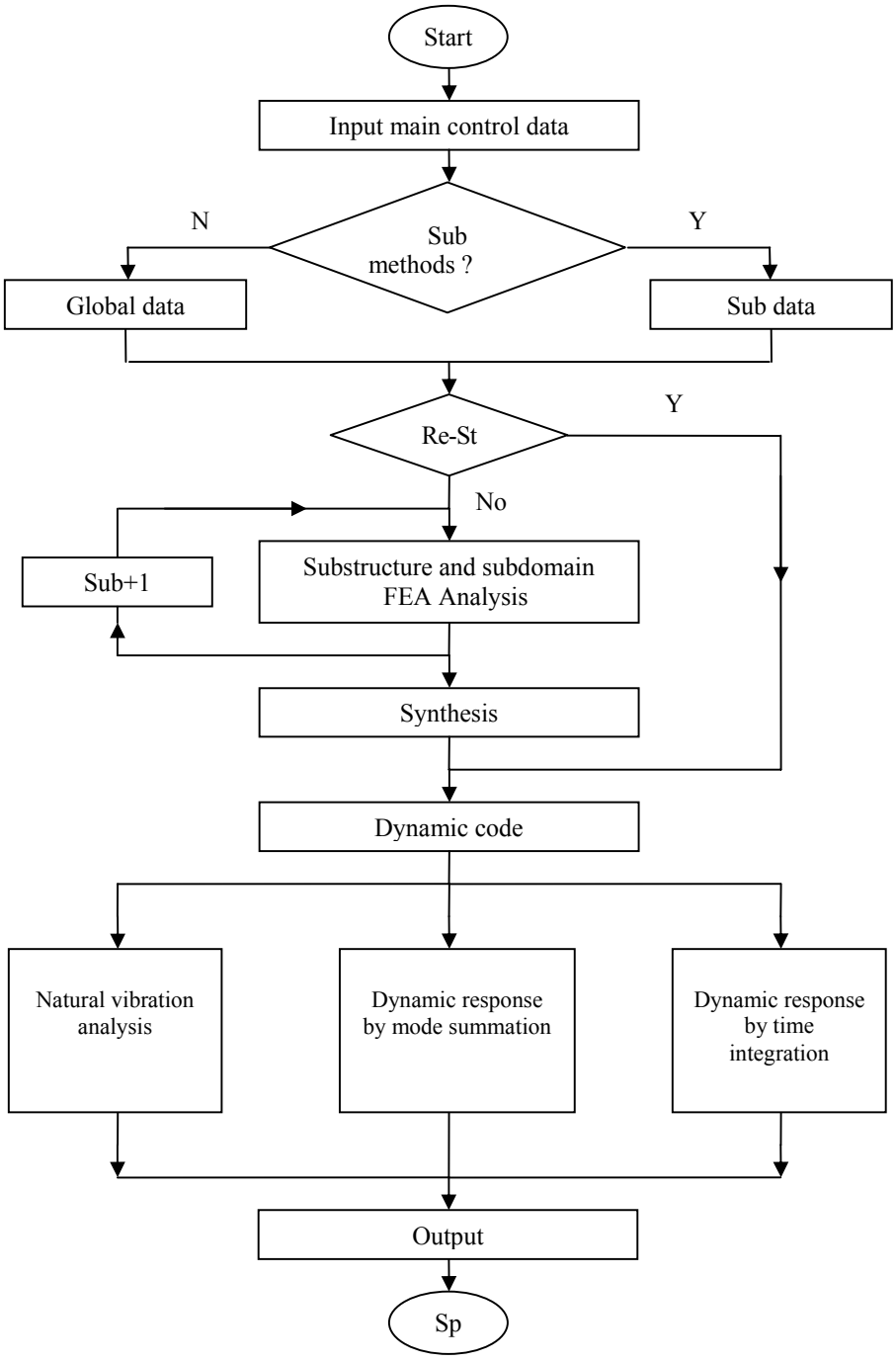

Fig.2.2 Main flow chart of computer program FSIAP

Chapter 3 Numerical Results: Natural Frequencies and Modes

3-1 General description

Coordinate system

As shown in Fig. 3.1, a Cartesian system O-xyz of origin at the centre of the tank is chosen as a global reference system in numerical analysis. All node positions used in this report are given under this coordinate system. The support points marked by the black dots in Fig. 3.1 are treated as fixed boundary to calculate the natural vibration characteristics.

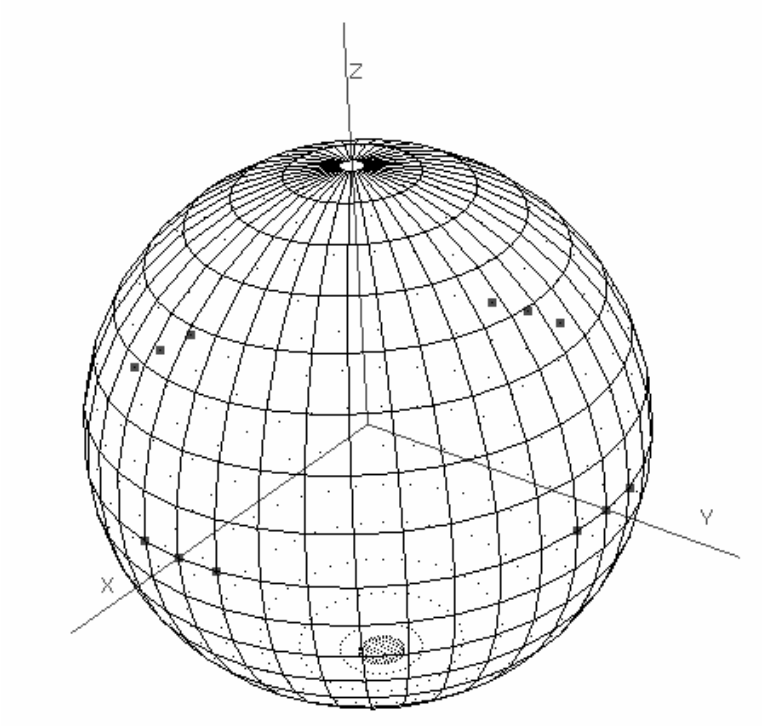

Fig. 3.1. The global coordinate system and the mesh structure of the solid tank

Finite element meshes

For the tank structure, 4 node plate – shell element is used as shown in Fig. 3.1 For the water domain, 8-node fluid pressure elements are used. Fig. 3.2 shows the mesh structure for the 50% water domain, where Fig. 3.2a) gives a view from a side direction of the ball and b) provides a view from the top of the tank.

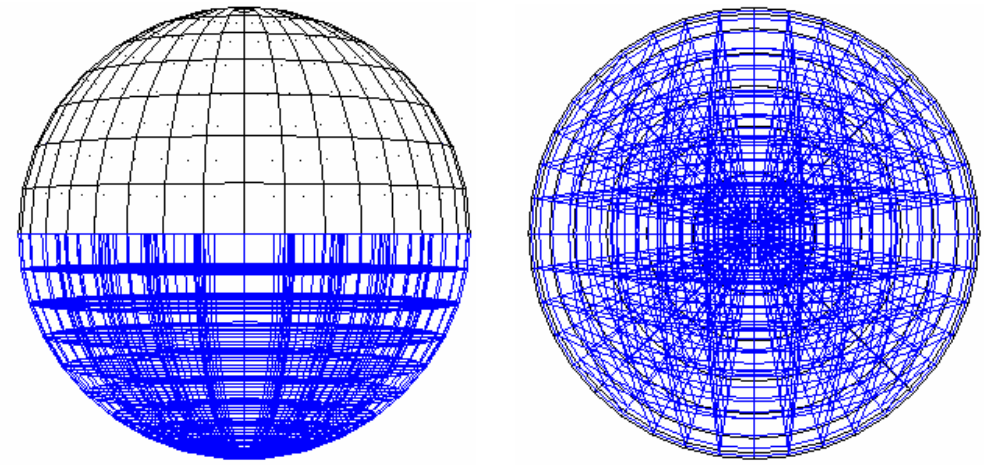

Fig. 3.2 The mesh structure of the water domain: a) a view from a side direction of the tank; b) a view from the top of the tanks

In this simulation, the solid tank is considered as a substructure and the water is treated as a fluid domain. The detailed element number, node number and the degree number of freedom used in the calculations are presented in the following sub-sections. More detailed data can be found in the data files given in the report.

Natural frequencies and modes

For each case, as mentioned in Chapter 1, the first 5 natural frequencies and the corresponding natural modes are listed in the following sub-sections of this chapter. The input files and output files for all cases are given in this report, from which more detailed data on the natural frequencies and modes can be read.

3-2 Empty Tank

FEA model

Number of nodal points	841
Number of plate-shell elements	820
Number of degree of freedom	4812
Number of natural frequencies and modes calculated	12

Natural frequencies (Hz)

mode = 1, freq. = 774.81000
mode = 2, freq. = 774.81000
mode = 3, freq. = 867.46997
mode = 4, freq. = 867.46997
mode = 5, freq. = 1143.40002

Natural modes: The first five natural modes are shown in Fig. 3.3 a)-e). The first mode and the second mode have same frequency 774.8Hz and show two sway motion forms along two horizontal directions. The third and fourth modes behave two roll motion forms about two horizontal directions. The fifth mode behaves a heave motion along the vertical direction.

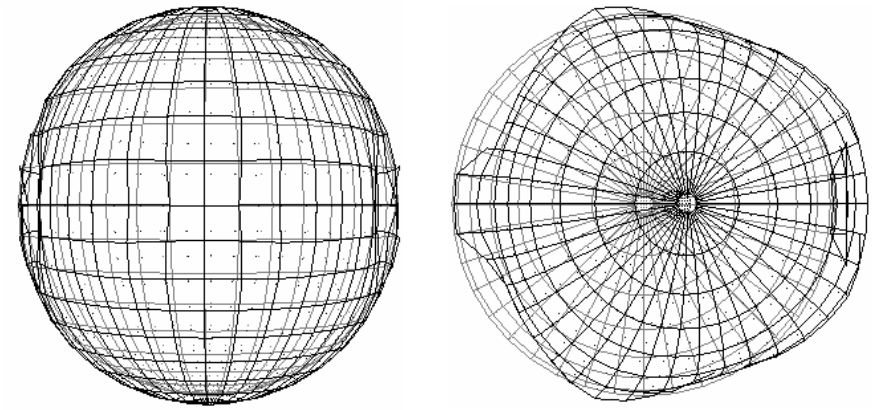

a) Mode 1 (774.8Hz): a sway vibration form in x-direction

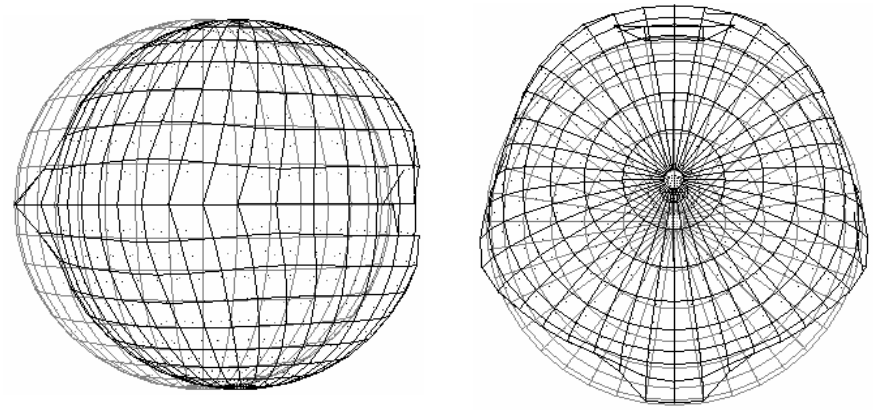

b) Mode 2 (774.8Hz): a sway vibration form in y-direction

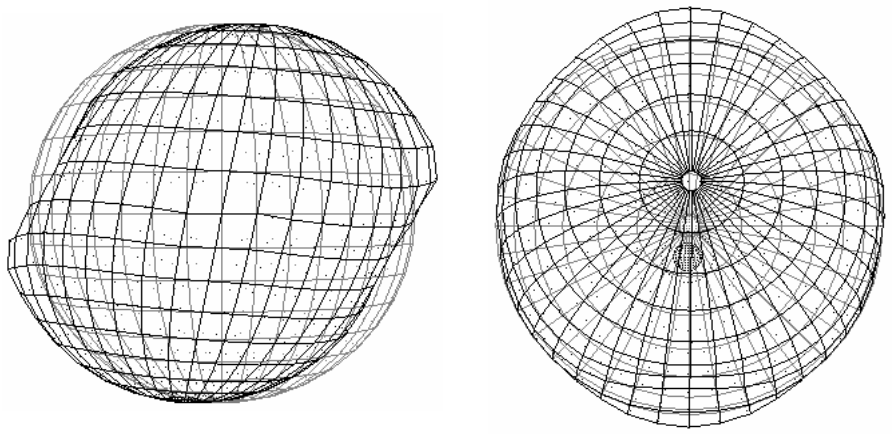

c) Mode 3 (867.5Hz): a roll vibration form about x-direction

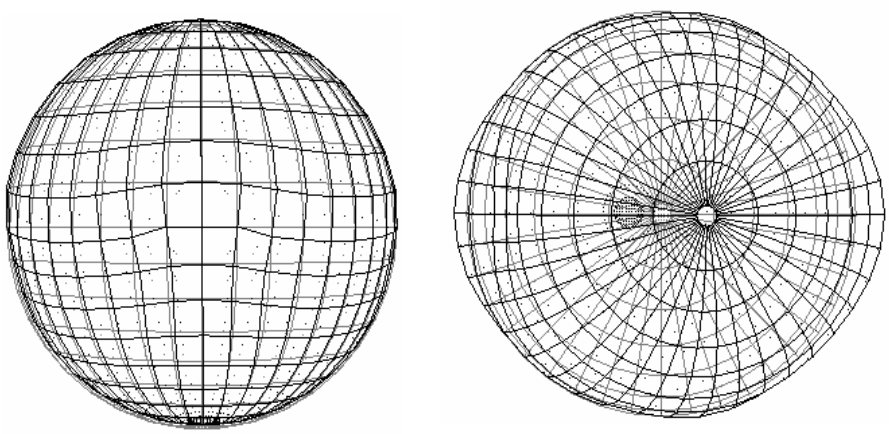

d) Mode 4 (867.5Hz): a roll vibration form about y-direction

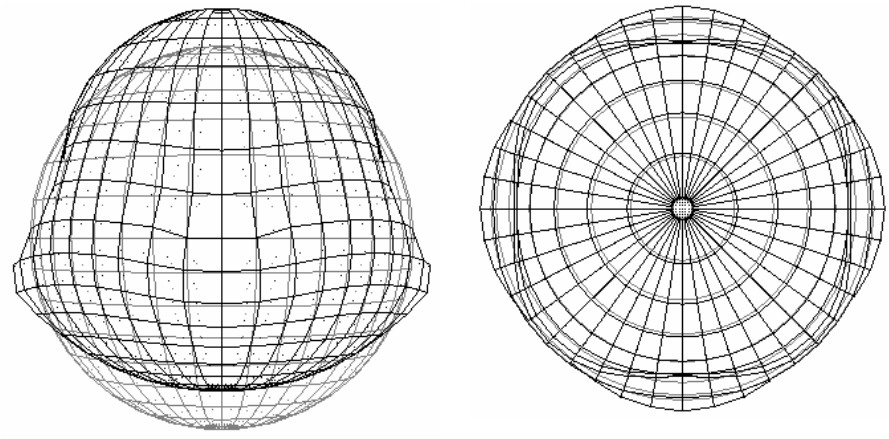

e) Mode 5 (1143.4Hz): a heave vibration form in z-direction

Fig. 3.3 The first natural modes of the empty tank

Experimental results

Fig 3.4 shows 5 curves obtained from the experiment. From these curves, we find the following peak frequencies: 633Hz, 656Hz, 674Hz, 773Hz, 768Hz, 814Hz and 832Hz. There is no experimental mode form data available to identify the mode for comparison with the calculations. However, the first natural frequency 774.8Hz calculated may be corresponds to 773Hz of experimental result.

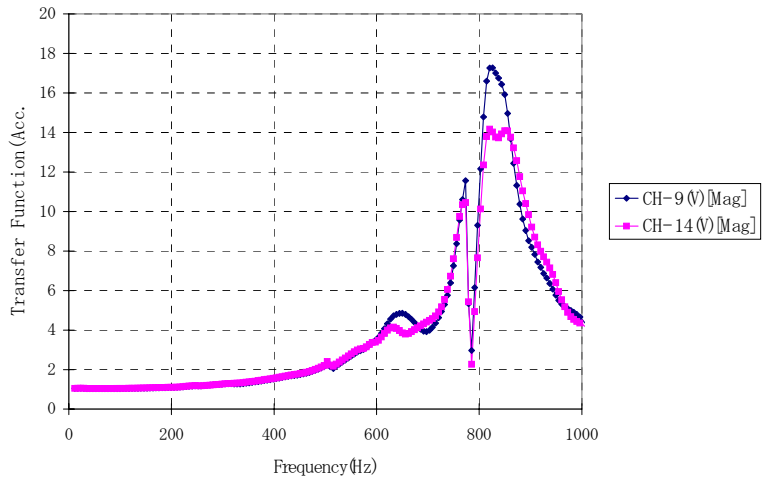

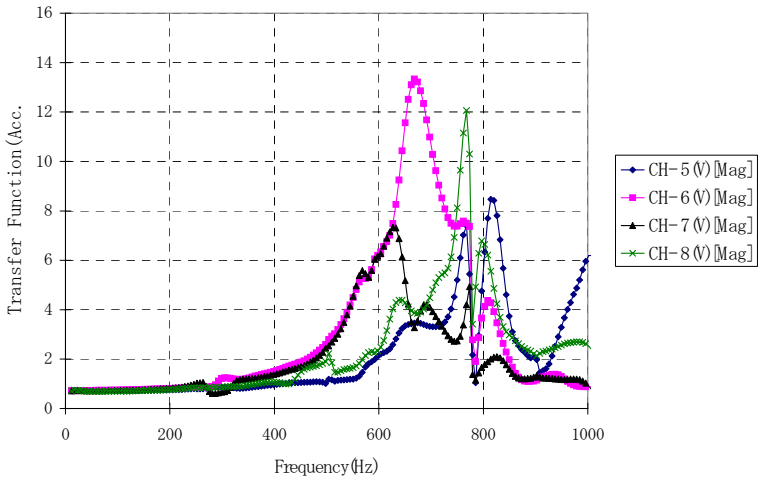

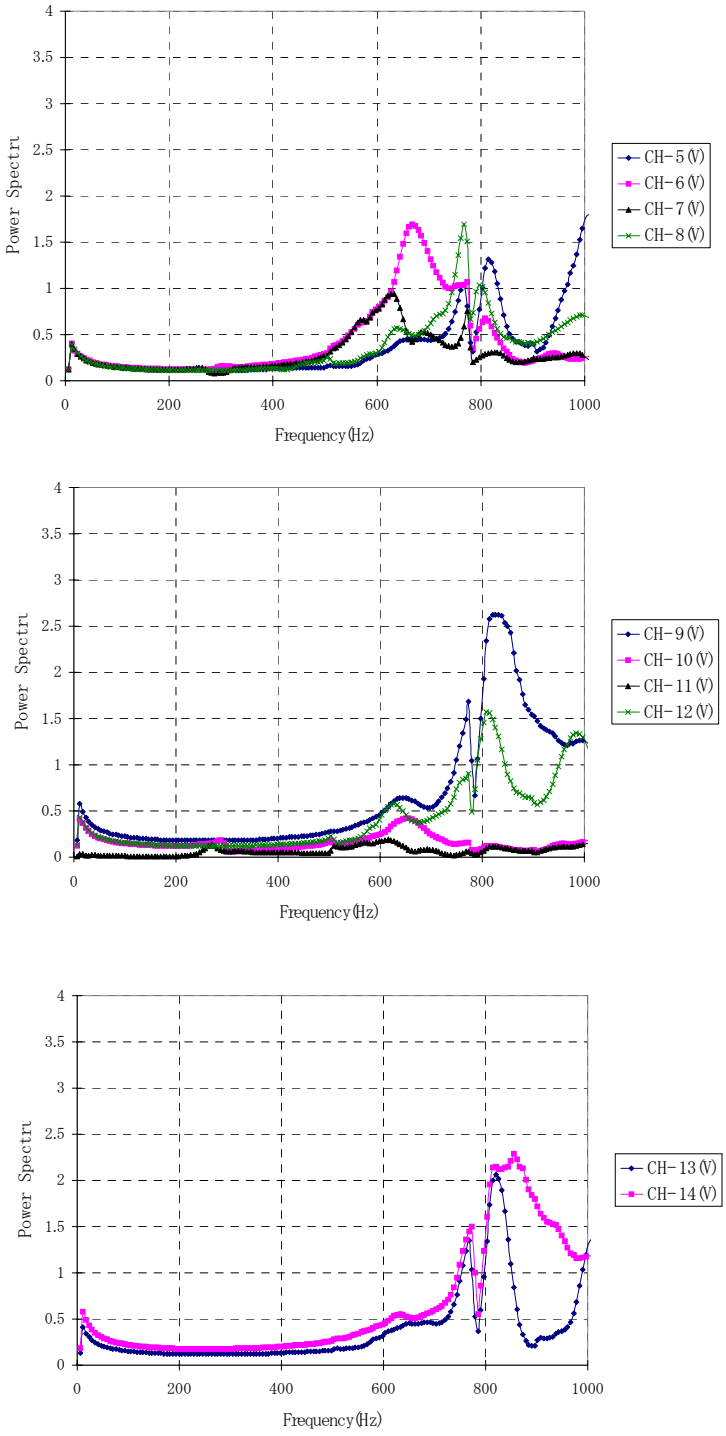

Fig. 3.4 Five curves obtained in the experiment

3-2 50% water filled tank with no free surface wave included

FEA model

Number of nodal points	1651
Number of plate-shell elements	820
Number of fluid elements	1000
Number of degree of freedom for solid	4813
Number of degree of freedom for fluid	1210
Number of natural frequencies and modes calculated	10

Natural frequencies (Hz)

mode = 1, freq. = 260.98999
mode = 2, freq. = 274.01999
mode = 3, freq. = 274.13000
mode = 4, freq. = 404.20999
mode = 5, freq. = 505.79999

Natural modes: The first five natural modes are shown in Fig. 3.5 a)-e). As shown in this figure, due to water-tank interactions, there are obvious changes of vibration modes. The first mode is now the heave motion mode with frequency 260.99Hz. The second and third modes have same frequency 274.02Hz and show two sway motion forms along two horizontal directions. Compared with the empty case, the motion of the tank bottom filled by water is larger than the top tank where no water filled. The fourth mode shows a compression and expansion motion form in two horizontal directions, respectively, and the tank bottom motion is bigger. The fifth mode behaves a more complex deformation.

a) Mode 1 (260.99Hz)

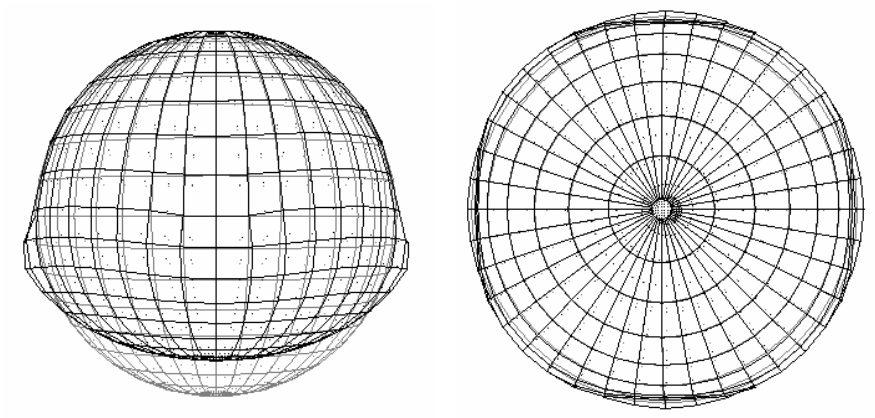

b) Mode 2 (274.02Hz)

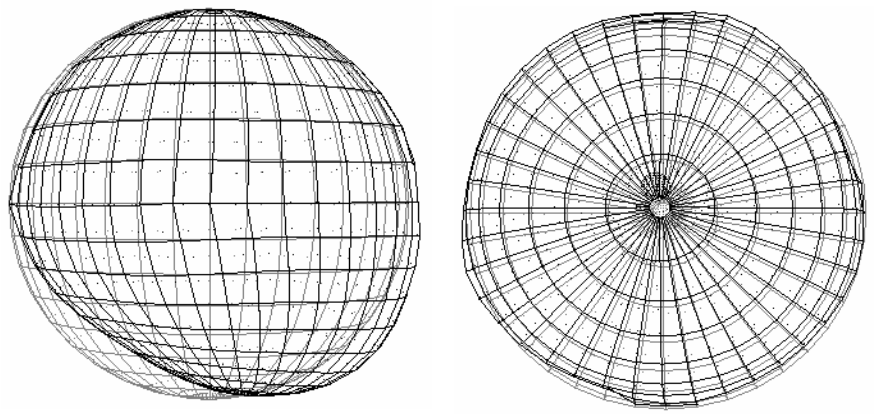

c) Mode 3 (274.13Hz)

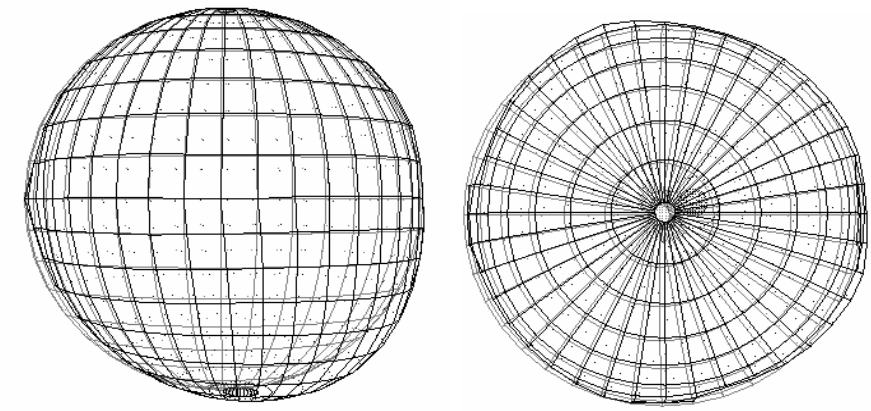

d) Mode 4 (404.21Hz)

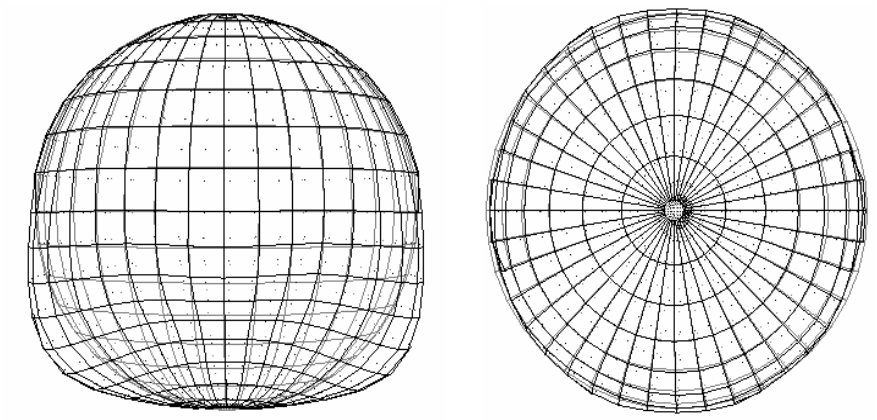

e) Mode 5 (505.80Hz)

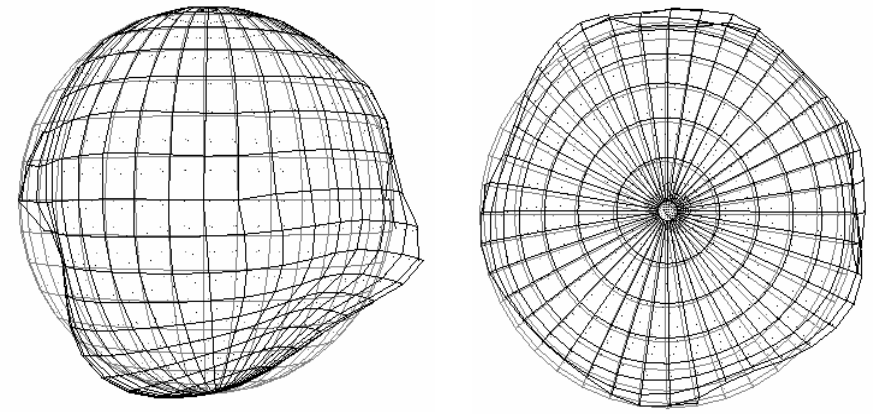

Fig. 3.5 The first five natural vibration modes obtained in simulations

Experiment Results

Fig. 3.6 presents three experimental curves measured at sensor 6 and 7. From these figures, there the following frequencies observe red: 270Hz, 311Hz, 533Hz, 656Hz and 662Hz. Here the frequency 270Hz is well agreed with the first calculation frequency of heave mode.

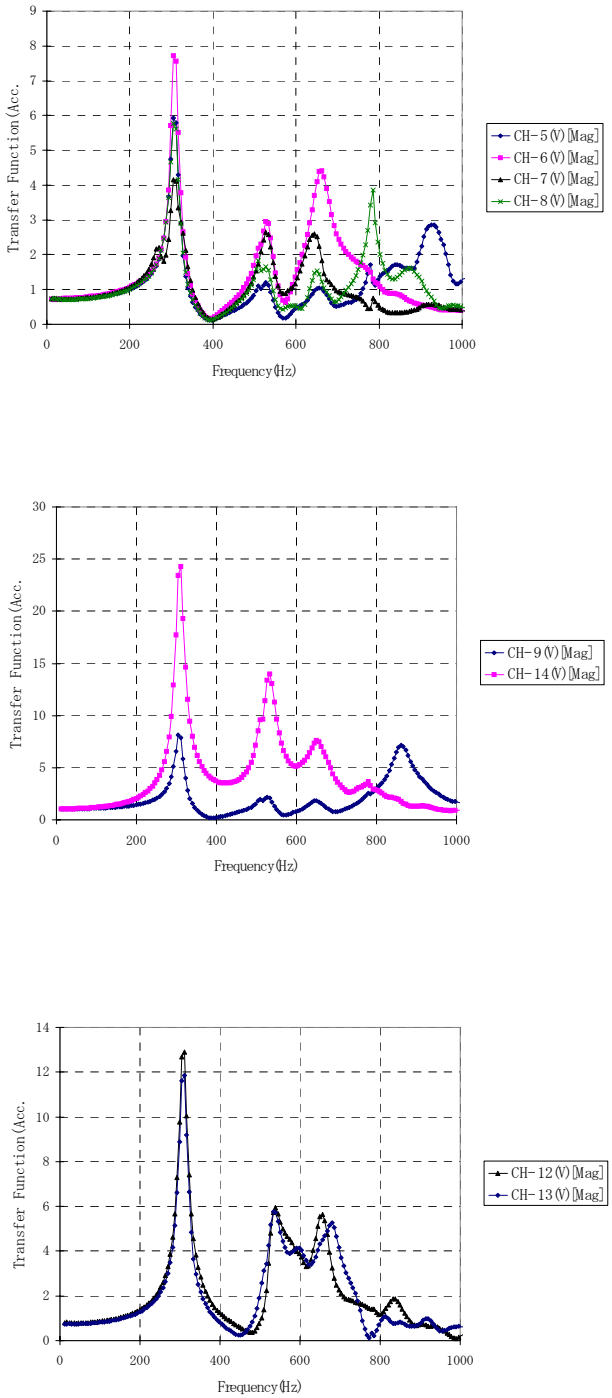

Fig. 3.6 Three experimental curves for 50% water tank with no free surface wave considered.

3-4 50% water filled tank with free surface wave considered

FEA model

Number of nodal points	1651
Number of plate-shell elements	820
Number of fluid elements	1000
Number of degree of freedom for solid	4813
Number of degree of freedom for fluid	1331
Number of natural frequencies and modes calculated	10

Natural frequencies (Hz)

mode = 1, freq. = 0.00000
mode = 2, freq. = 1.62480
mode = 3, freq. = 1.62480
mode = 4, freq. = 2.20130
mode = 5, freq. = 2.20640

Natural modes: The first five natural modes are shown in Fig. 3.7 a)-e). Due to the free surface wave is considered, the natural frequencies of the system are much lower than the case of neglecting free surface wave. The main modes of the system are sloshing modes. As shown in this figure. The first mode is a static mode with zero frequency which is similar to the rigid mode of structure vibration. The second and third modes have same frequency 1.6248Hz and show two sloshing motions. The fourth and fifth modes show two similar modes with frequency about 2.2Hz.

a) Mode 1 (0Hz) Constant pressure mode

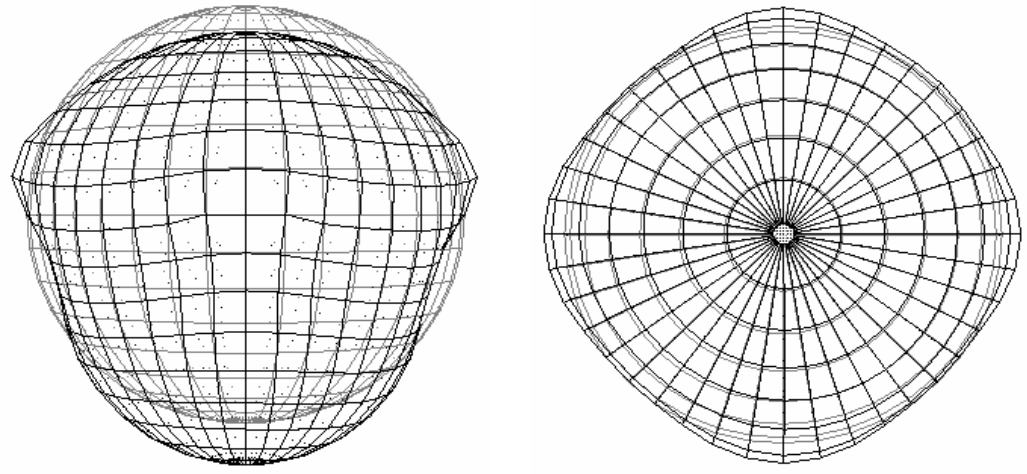

b) Mode 2 (1.625Hz)

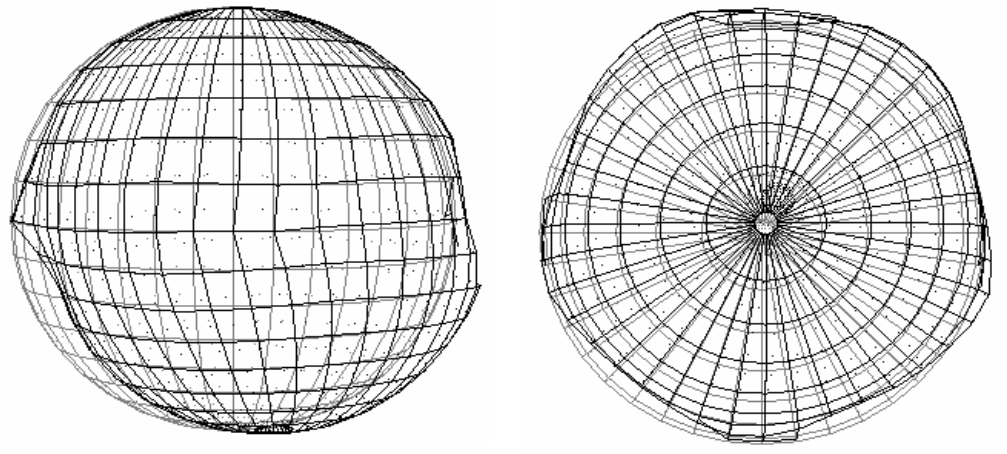

c) Mode 3 (1.625Hz)

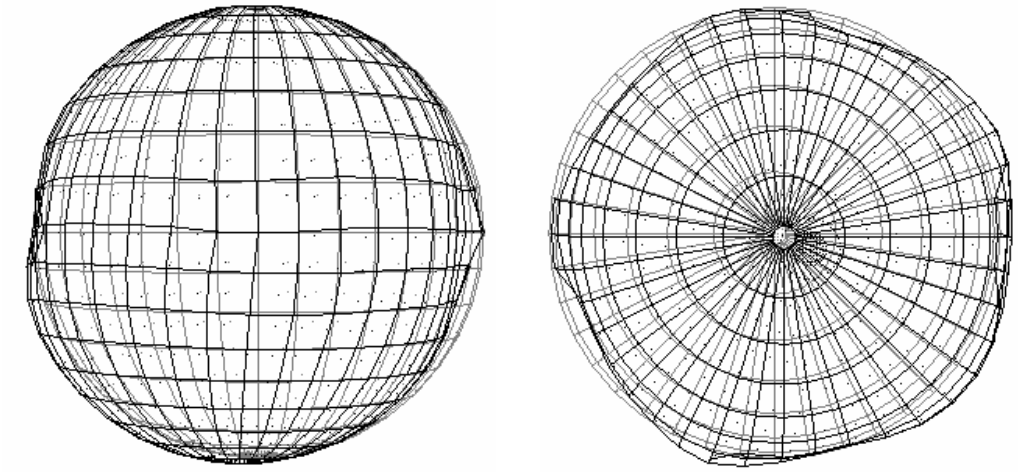

d) Mode 4 (2.20Hz)

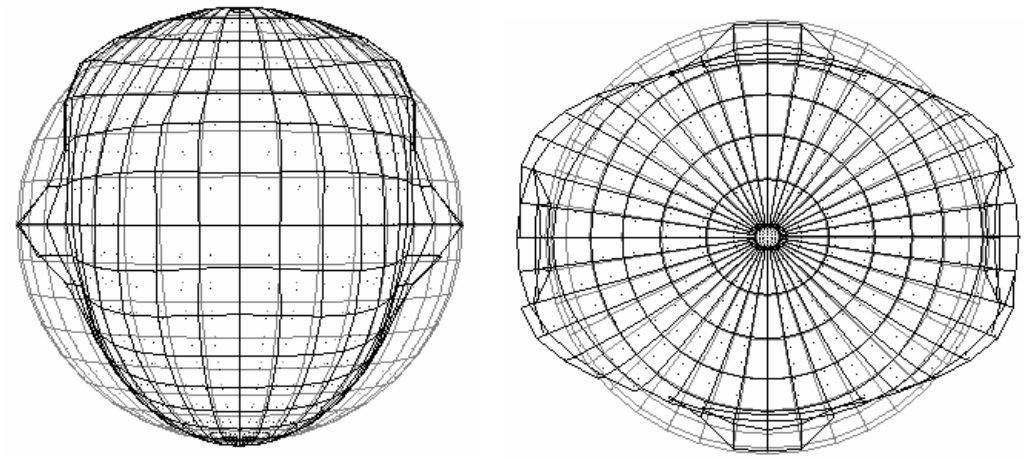

e) Mode 5 (2.21Hz)

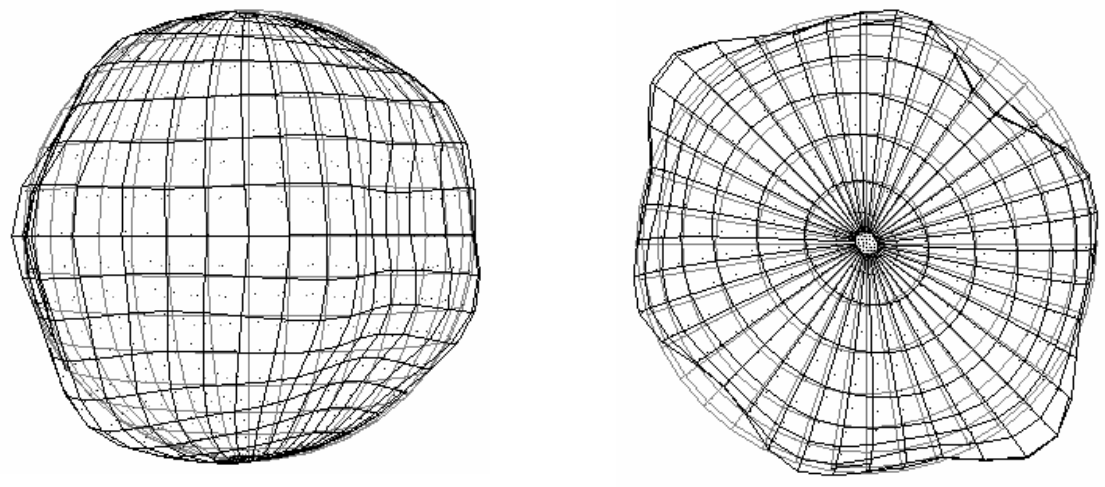

Experimental results Not available.

3-5 66% water filled tank

FEA model

Number of nodal points	1853
Number of plate-shell elements	860
Number of fluid elements	1200
Number of degree of freedom for solid	5053
Number of degree of freedom for fluid	1452
Number of natural frequencies and modes calculated	10

Natural frequencies (Hz)

mode = 1, freq. = 246.06000
mode = 2, freq. = 246.06000
mode = 3, freq. = 252.28000
mode = 4, freq. = 381.92999
mode = 5, freq. = 431.64999

Natural modes: The first five natural modes are shown in Fig. 3.8 a)-e). The first and second modes have a same frequency 246.06Hz with the motion forms similar to the 2nd and 3rd modes in the 50% water case. The third mode is the heave motion mode with frequency 252.28Hz. The fourth mode of frequency 381.93Hz and the fifth mode of frequency 431.65Hz are similar to the ones for the case of 50% water filed tank.

a) Mode 1 and b) Mode 2 (246.06Hz)

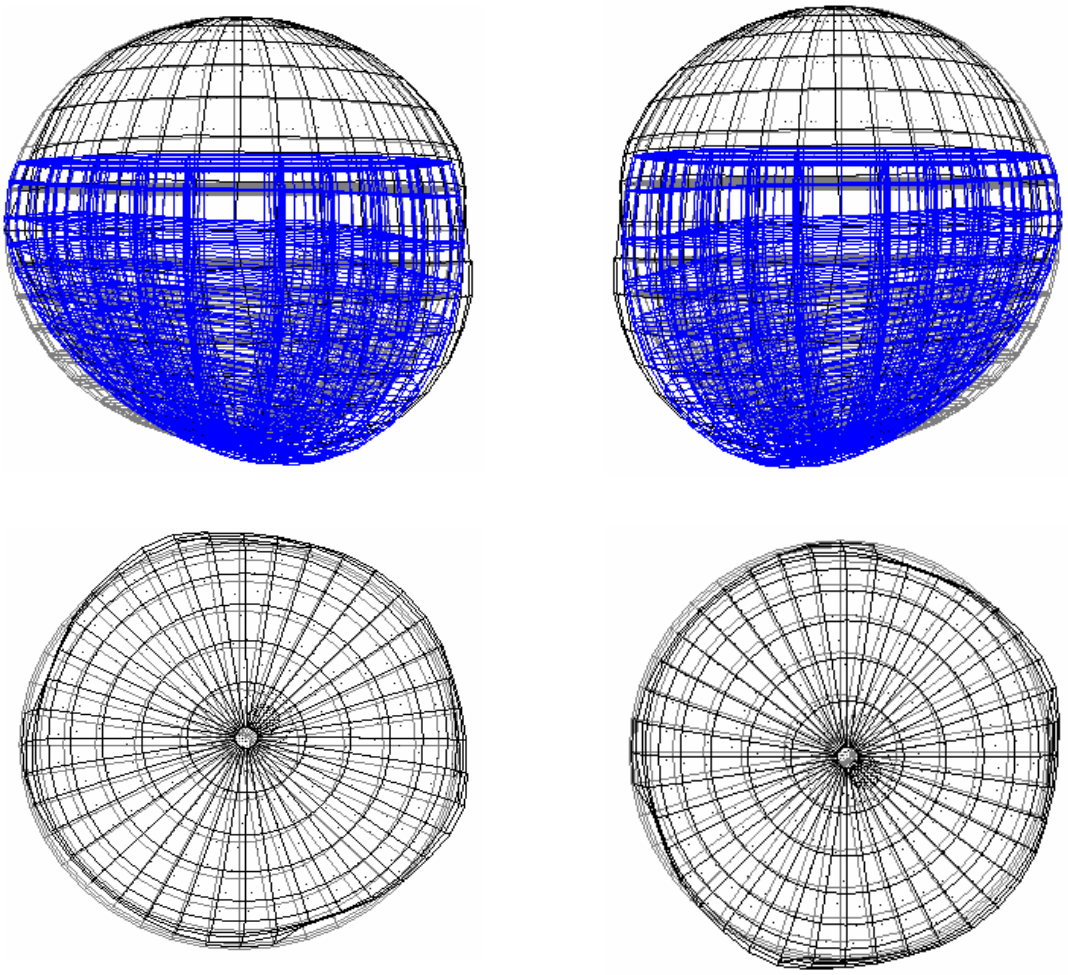

b) Mode 3 (252.28Hz)

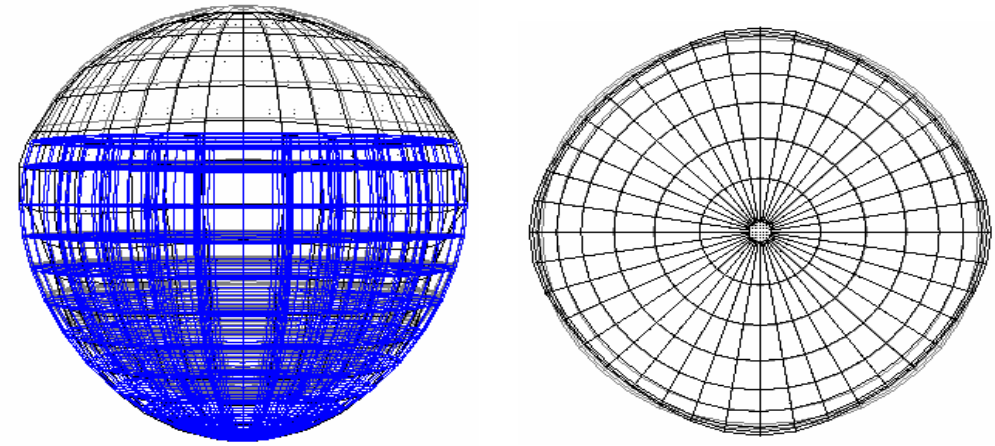

d) Mode 4 (381.93Hz)

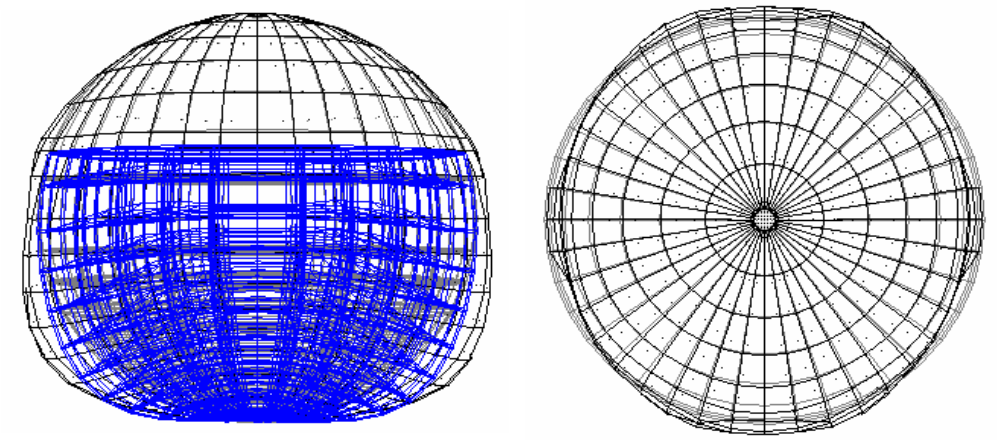

e) Mode 5 (431.65Hz)

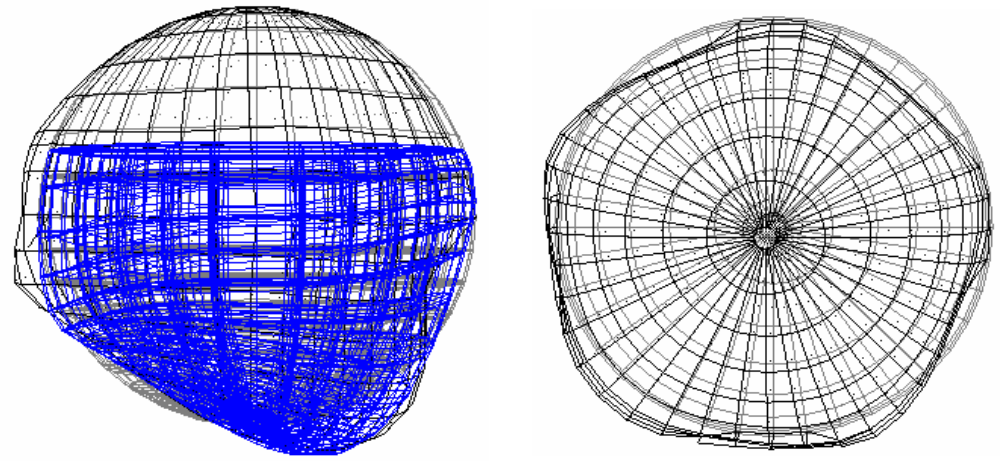

Fig. 3.8 The first five natural modes of 66% water filed tank

Experiment Results

Fig. 3.9 shows three curves obtained in the experiment, from which three frequencies are found**:** 275Hz, 469Hz and 480Hz.

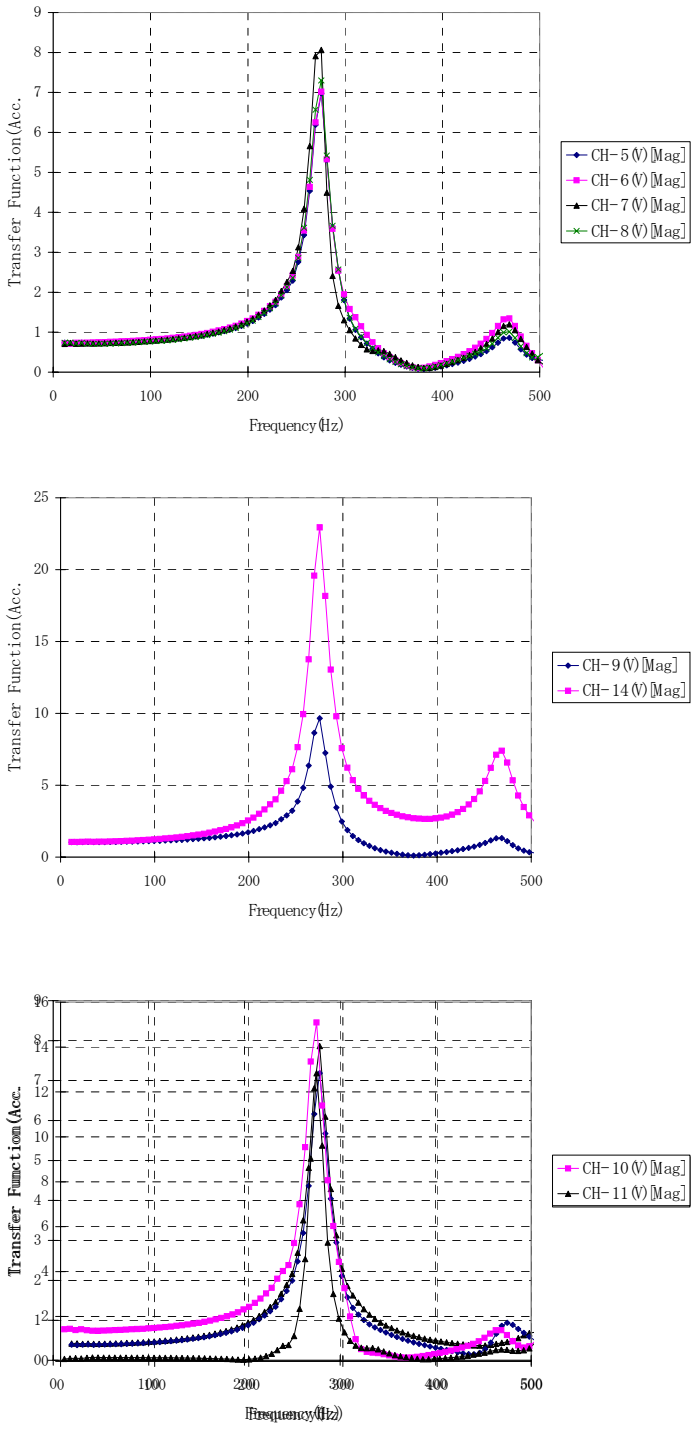

Fig. 3.9 The three curves obtained in the experiment

3-6 Fully filled tank

FEA model

Number of nodal points	2299
Number of plate-shell elements	820
Number of fluid elements	1800
Number of degree of freedom for solid	4837
Number of degree of freedom for fluid	2178
Number of natural frequencies and modes calculated	10

Natural frequencies (Hz)

mode = 1, freq. = 196.66000
mode = 2, freq. = 196.66000
mode = 3, freq. = 201.24001
mode = 4, freq. = 322.81000
mode = 5, freq. = 326.89001

Natural modes: The first five natural modes are shown in Fig. 3.10 a)-e). The first and second modes have an approximately same frequency 196.6 Hz with the motion forms similar to the 2nd and 3rd modes in the 50% and 66% water cases. The third mode is the heave motion mode with frequency 201.2Hz. The fourth mode of frequency 322.8Hz and the fifth mode of frequency 326.89Hz are similar to the ones for the cases of 50% and 66% water filed tank.

Mode 1 (196.6Hz)

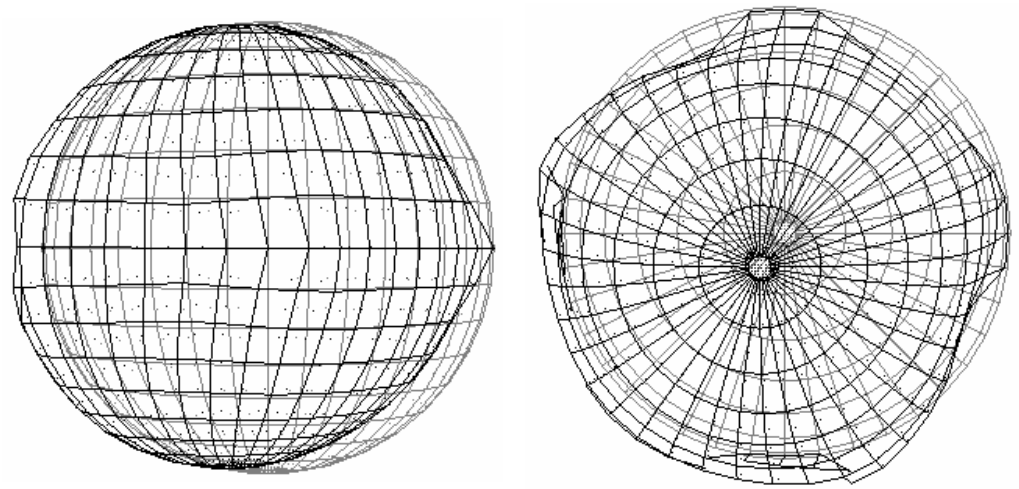

Mode 2 (196.7Hz)

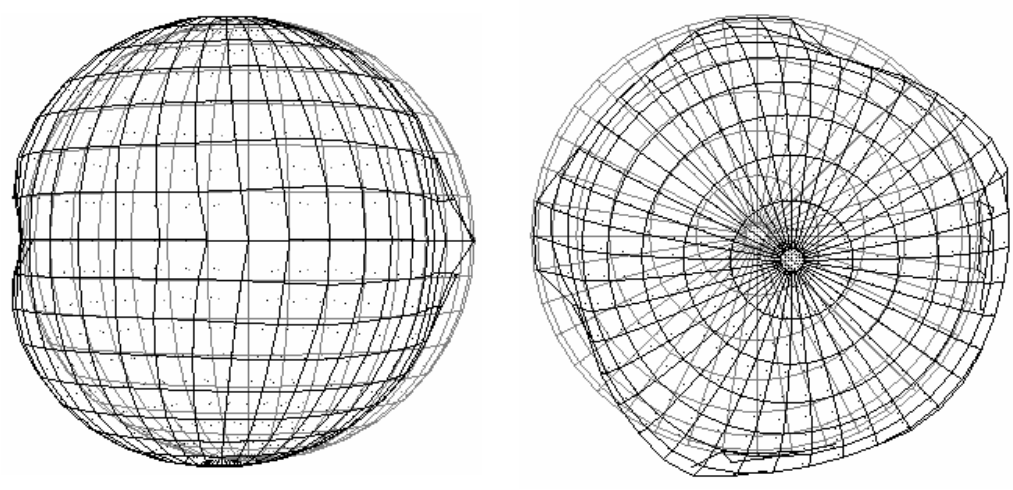

Mode 3 (201.2Hz)

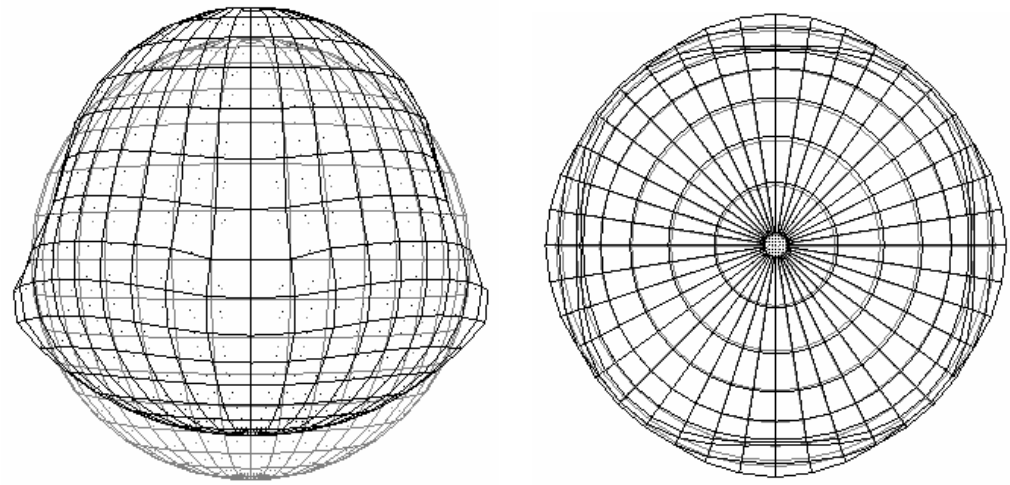

Mode 4 (322.8Hz)

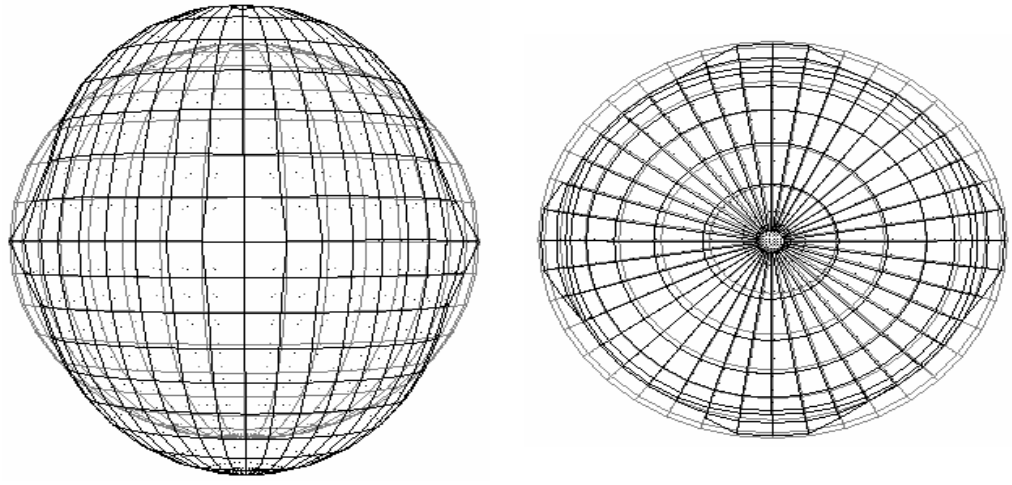

Mode 5 (326.89Hz)

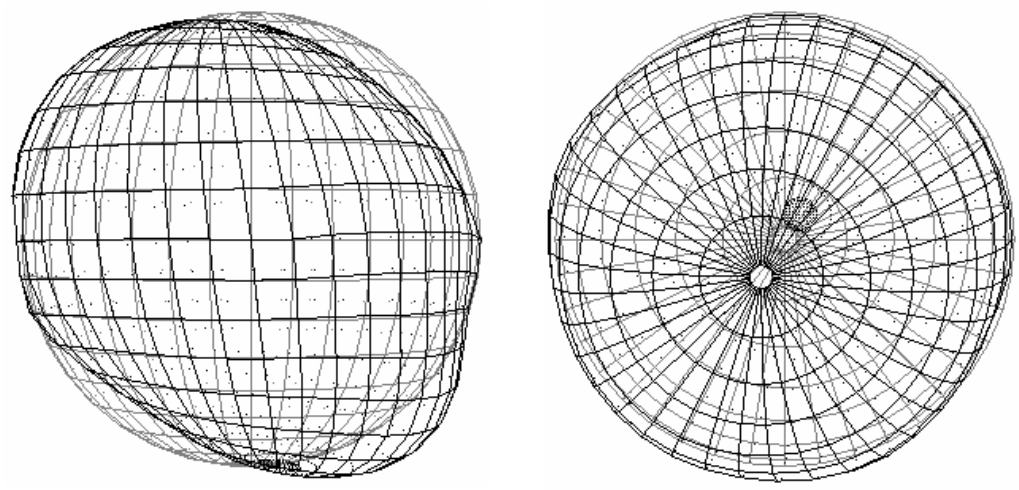

Fig. 3.10 The first five natural modes for 100% water filled tank.

Experimental results

Fig. 3.11 gives three curves obtained in the experiment from which three peak frequencies are found: 258Hz, 387Hz and 475Hz.

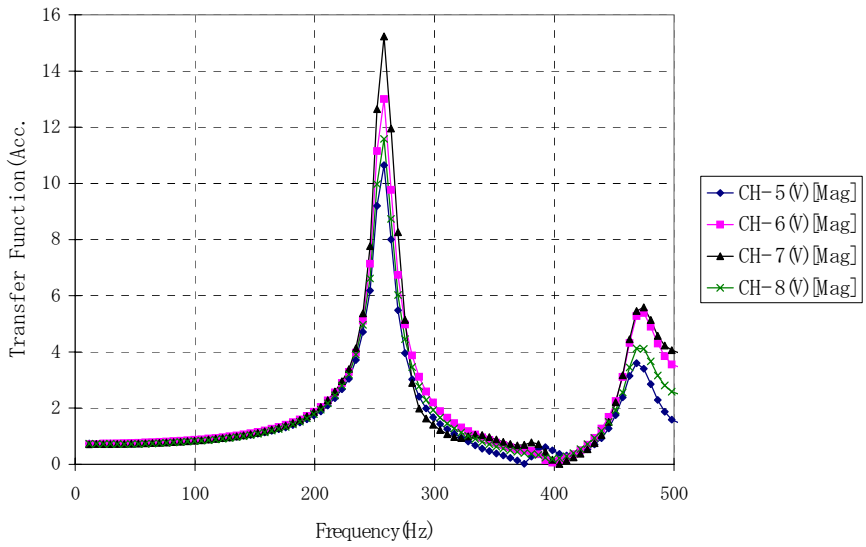

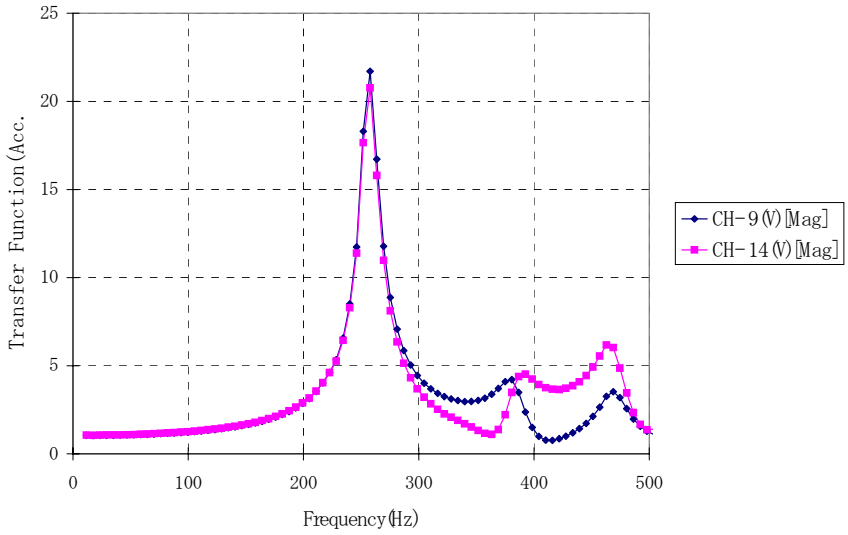

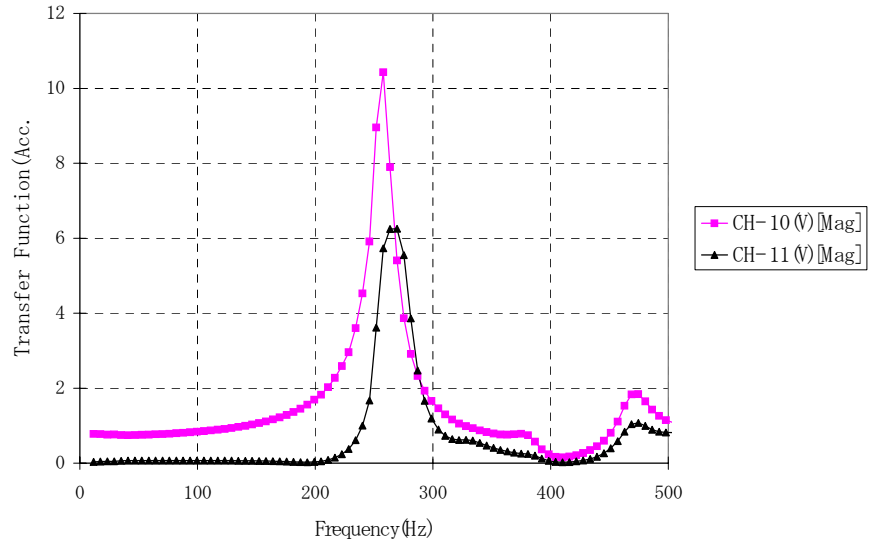

Fig. 3.11 Three curves obtained in the experiment

3-7 The effect of filled water level on the natural frequencies

Table 3.1 listed the natural frequencies obtained in the calculations which are arranged according to the identified mode shapes. Fig. 3.12 gives a curve to show the effect of the water level on the heave natural frequency. To better to study the water level effect, the first three frequencies of 25% water level tank, which is not required in the contract, are added.

Table 3.1 The effect of filled water level on the natural frequencies (Hz)

Mode	0% water	25% water	50% water	66.7% water	100% water
Heave	1143.4	335.8	260.99	252.28	201.2
Sway	774.8	502.1	274.13	246.06	196.6
Sway	774.8	502.1	274.13	246.06	196.7
	867.5*		404.21	381.95	322.8
	867.5*		505.80	431.65	326.89

*Note: These two mode frequencies obtained for the empty tank case are listed here for a reference only because the mode shapes are different if compared with the cases of filled water.

From Table 3.1 and Fig. 3.12 as well as the results presented in this chapter, we may conclude that:

1) The filled water change the order of vibration mode, such as, the heave mode is the fifth mode for the empty case but is the first mode for 50% water level case and the third mode for 66% and 100% water level cases.

2) There is a significant decrease of the natural frequencies due to 25% filled water. However, after the filled water level higher that 25%, the increase of water level does not significantly decrease the natural frequencies of similar vibration mode shapes.

3) The decrease gradient of the natural frequency as a function of water level tends to small constant.

4) It is not possible that there is a zero natural frequency for any water level filled tank with no free surface wave considered.

5) The free surface wave effect causes a lot of water sloshing modes with very lower frequencies than the natural frequencies of the dry tank structure.

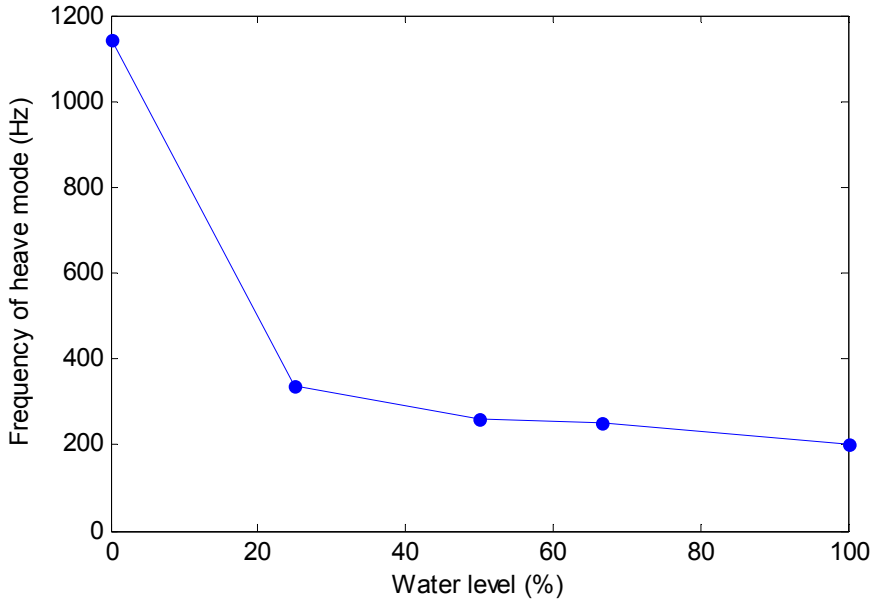

Fig. 3.12 The effect of water level on the natural frequency of the heave vibration mode of water-tank interaction system

3-8 Discussion on the comparison with experimental results

The numerical results and some experimental results have been presented in previous sections of studied cases to provide a comparison. As mentioned in the related sections, we can say that the important frequencies obtained in the numerical simulations are basically agreeable with the experiment results. However, the following factors are needed to be considered to understand the possible error in both numerical and experimental process.

Boundary condition of tank support

In the numerical model, the tank is ideally fixed at three points of each support part as shown in Fig. 3.1. It was investigated that fixed four rectangle area of the shell surface on where four supports are connected does not make any obvious change for natural frequencies of the empty tank. In the experimental device, these four support parts are fixed by bolts, of which the stiffness of support is affected by the bolt forces. These non-fully determined factors are difficult to be simulated in the numerical model.

Additional mass and stiffness of sensors

The additional mass and stiffness of sensors are not considered in the numerical model to provide the numerical results for real product analysis use.

Mode shape identification

To measure the natural frequencies and the corresponding modes, the use of resonance test equipment is necessary. It is very difficult to measure vibration mode shapes which are affected by the phase of vibration signals measured using vibration table test. We have not got mode shape experiment results, and therefore it is difficult to identify the suitable mode to compare the results.

Chapter 4 Numerical Results: Dynamic Responses

4-1 General description

In the dynamic response analysis, the tank system is excited by a vertical sinusoidal motion of acceleration amplitude 1g, i.e. 981cm/s^2. The damping coefficients of the modes used in the calculations are listed in Table 4.1. The output points of displacement or pressure responses and their correspondence to the sensors position are listed in Table 1.1-1.5. The notations of output responses in the output data files are given in section 2-3. The mesh and FEA model of numerical calculation for each case are same as the analysis of natural vibration calculations presented in the chapter 3.

Table 4.1 Damping coefficients used in the calculations of dynamic responses. The data is provided from the experiment curves calculated by IHI representative

Case	Empty	50%	67%	100%
Exp.No	No.4	No.7	No.9	No.16
Ch.No	No.9	No.14	No.14	No.14
Frequency (Hz)	826	311	275	258
Peak value	17.3	24.3	22.9	20.3
0.707 Peak value	12.2	17.2	16.2	14.4
Half-power band width	65	20	16	16
ζ	**0.039**	**0.032**	**0.029**	**0.031**

In this report, the displacement or pressure response curves at selected points are plotted for each case. The maximum response amplitudes are listed in the tables. The more detailed data can be read in the output data flies including in the report.

4-2 Empty Tank

For the empty case, the frequency of heave mode is 1143.4Hz of which the damping confident is not provided, but the damping 0.039 is still used in dynamic response calculation.

Base motion

Frequency 1143.4Hz

Acceleration amplitude 1g = 981cm/s^2

Related data in calculation

Retained mode number	145
Maximum frequency of retained modes	2316.4Hz
Damping coefficient	0.039
Time step	0.00005s
Calculation time step	300
Output step interval	2

Table 4.2 shows the maximum amplitudes at interest points and arriving times. Fig. 4.1 shows the displacement response curves at top sensor point 9 and the bottom sensor point 14.

Table 4.2 Maximum displacement values and arriving time at interest points

Node-(component)	61-(1)	61-(2)	61-(3)	292-(1)	292-(2)	292-(3)
Values (cm)	3.868375D-08	4.186292D-08	2.797310D-04	1.082624D-05	1.083551D-05	1.756679D-04
Time (s)	7.000000D-04	7.000000D-04	1.450000D-02	1.410000D-02	1.410000D-02	1.230000D-02
Node-(component)	321-(1)	321-(2)	321-(3)	642-(1)	642-(2)	642-(3)
Values (cm)	1.081265D-05	1.081368D-05	1.756827D-04	1.140755D-05	1.140836D-05	1.713505D-04
Time (s)	1.410000D-02	1.410000D-02	1.230000D-02	1.410000D-02	1.410000D-02	1.230000D-02
Node-(component)	652-(1)	652-(2)	652-(3)	671-(1)	671-(2)	671-(3)
Values (cm)	1.138431D-05	1.138050D-05	1.713607D-04	1.140193D-05	1.139497D-05	1.713468D-04
Time (s)	1.410000D-02	1.410000D-02	1.230000D-02	1.410000D-02	1.410000D-02	1.230000D-02
Node-(component)	681-(1)	681-(2)	681-(3)	836-(1)	836-(2)	836-(3)
Values (cm)	1.138621D-05	1.138791D-05	1.713614D-04	5.589613D-09	3.348093D-06	2.736102D-04
Time (s)	1.410000D-02	1.410000D-02	1.230000D-02	1.800000D-03	1.320000D-02	1.100000D-02

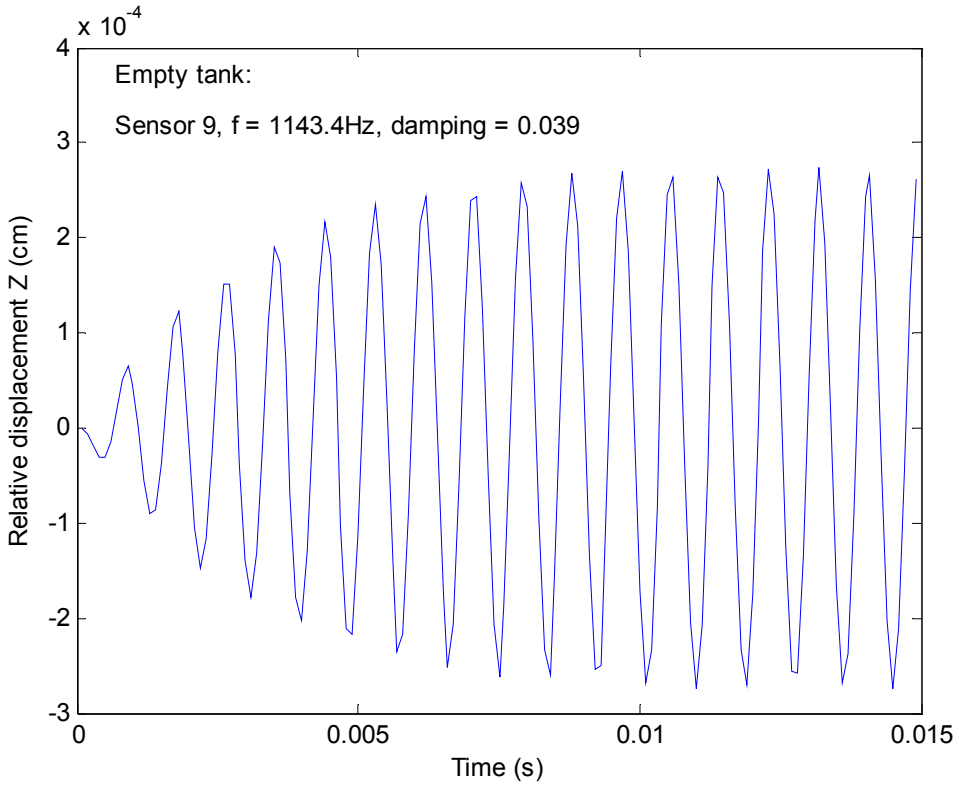

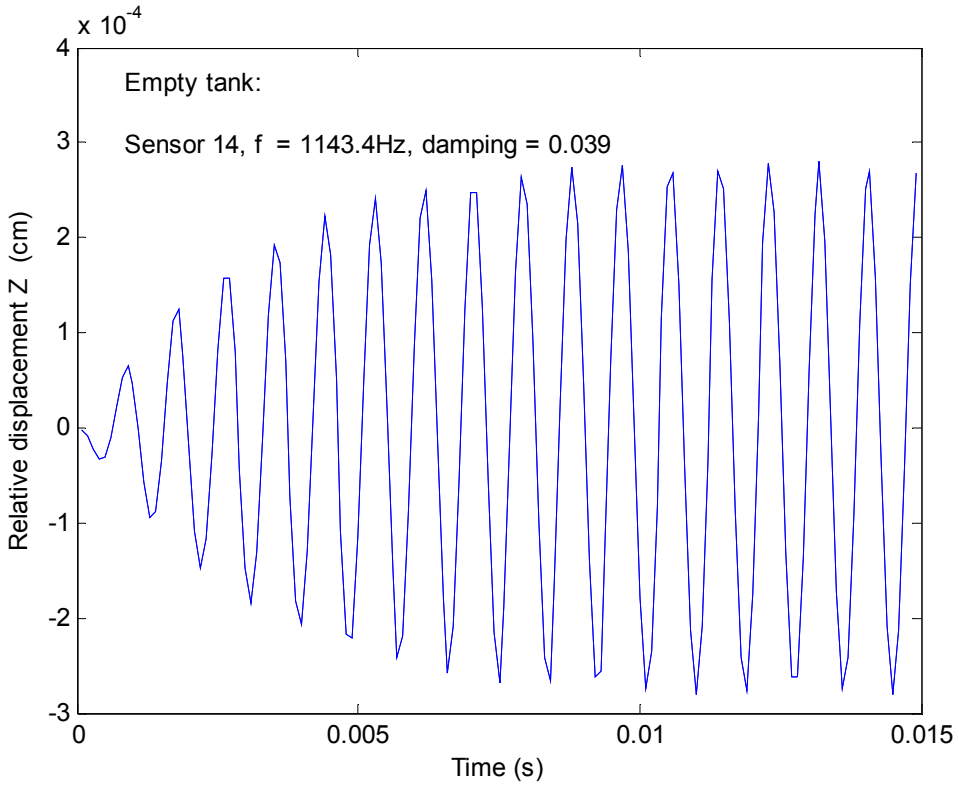

Fig. 4.1 The time response histories in z-direction at top sensor 9 and bottom sensor 14 of the tank

4-3 50% water filled with no free surface wave

Base motion

Frequency 260.99Hz

Acceleration amplitude 1g = 981cm/s^2

Related data in calculation

Retained mode number 10

Maximum frequency of retained modes 681.16Hz

Damping coefficient 0.032

Time step 0.0002s

Calculation time step 300

Output step interval 2

Table 4.3 shows the maximum amplitudes at interest points and arriving times. Fig 4.4 shows the pressure response at points 16a) and 16b). Fig. 4.5 shows the displacement response curves at top sensor point 9 and the bottom sensor point 14.

Table 4.3 Maximum displacement and pressure values and arriving time at interest point

Node-(component)	61-(1)	61-(2)	61-(3)	212-(1)	212-(2)	212-(3)
Values (cm)	5.501976D-05	3.664841D-05	7.195841D-03	9.924487D-05	1.454330D-04	5.668927D-03
Time (s)	5.440000D-02	5.440000D-02	5.200000D-02	4.600000D-02	5.400000D-02	5.200000D-02
Node-(component)	252-(1)	252-(2)	252-(3)	292-(1)	292-(2)	292-(3)
Values (cm)	1.277538D-04	8.785984D-05	4.687921D-03	4.571541D-04	4.386536D-04	3.712082D-03
Time (s)	5.600000D-02	5.000000D-02	5.200000D-02	5.400000D-02	5.200000D-02	5.200000D-02
Node-(component)	321-(1)	321-(2)	321-(3)	642-(1)	642-(2)	642-(3)
Values (cm)	4.667969D-04	4.521958D-04	3.750491D-03	3.077547D-05	2.817997D-05	8.320097D-04
Time (s)	5.400000D-02	5.400000D-02	5.200000D-02	5.440000D-02	5.240000D-02	5.960000D-02
Node-(component)	652-(1)	652-(2)	652-(3)	671-(1)	671-(2)	671-(3)
Values (cm)	3.774747D-05	2.342599D-05	8.055954D-04	2.529829D-05	4.091305D-05	8.073486D-04
Time (s)	5.240000D-02	1.200000D-03	5.960000D-02	1.200000D-03	5.240000D-02	5.960000D-02
Node-(component)	681-(1)	681-(2)	681-(3)	836-(1)	836-(2)	836-(3)
Values (cm)	2.624061D-05	2.994771D-05	7.824668D-04	1.489080D-05	1.545223D-05	8.043945D-04
Time (s)	5.240000D-02	5.240000D-02	5.960000D-02	5.800000D-02	5.400000D-02	5.200000D-02
Node-(component)	871-(7)	1022-(7)	1062-(7)	1102-(7)	1131-(7)	
Values (kg/cm2)	2.342820D-01	1.732077D-01	1.361906D-01	9.834280D-02	9.782718D-02	
Time (s)	5.200000D-02	5.200000D-02	5.200000D-02	5.960000D-02	5.960000D-02	

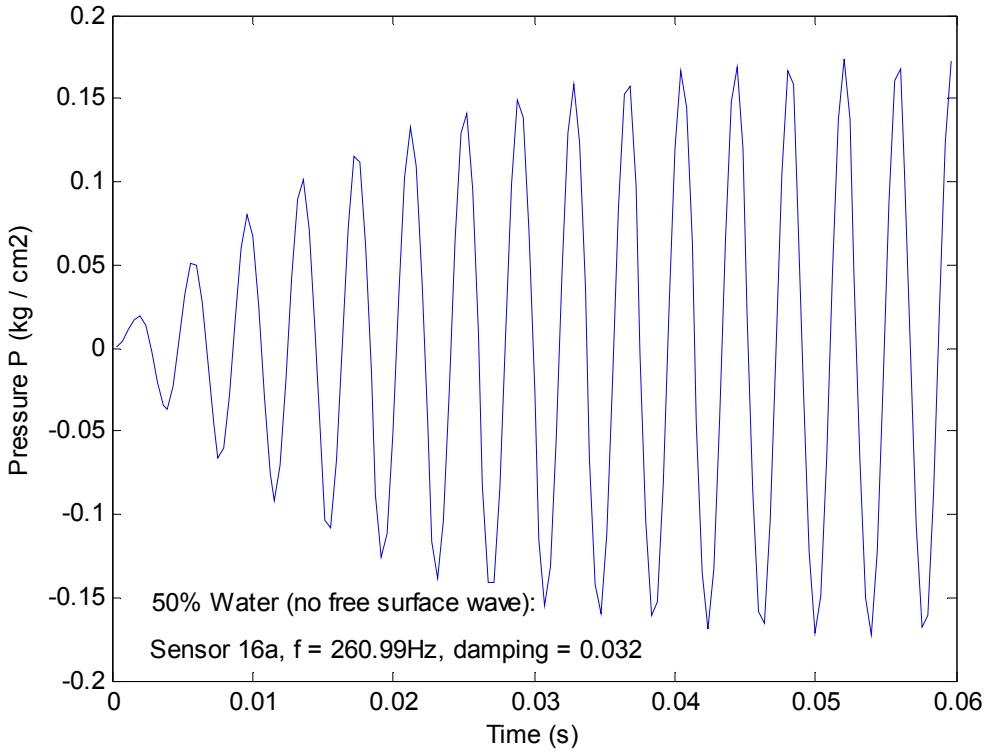

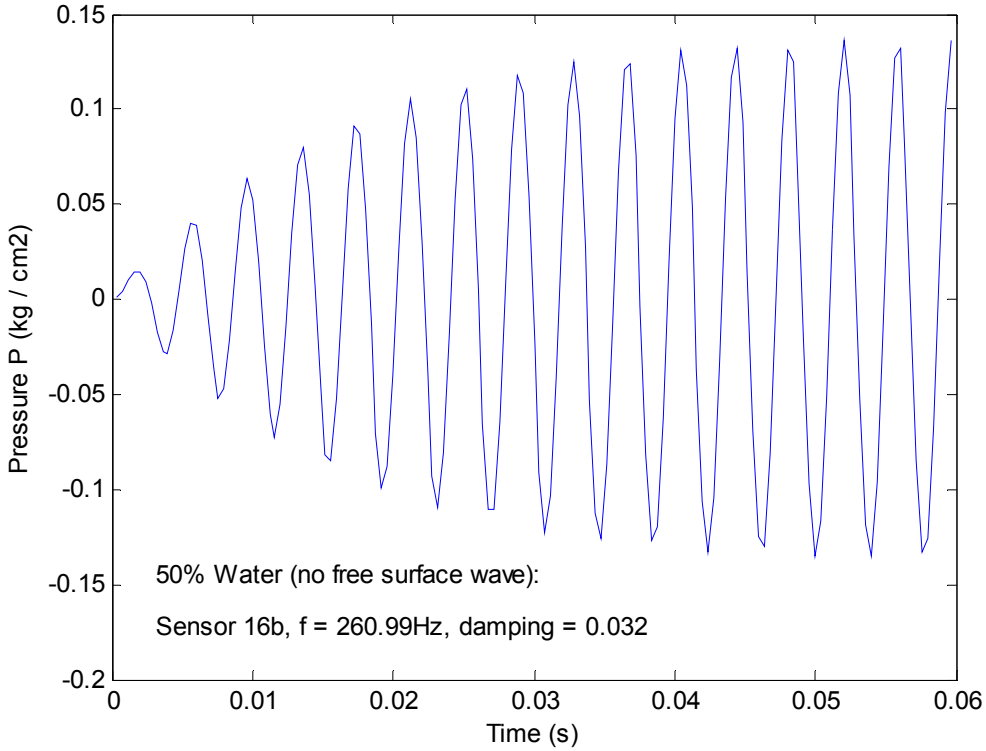

Fig. 4.4 The time response histories at point 16a) and 16b).

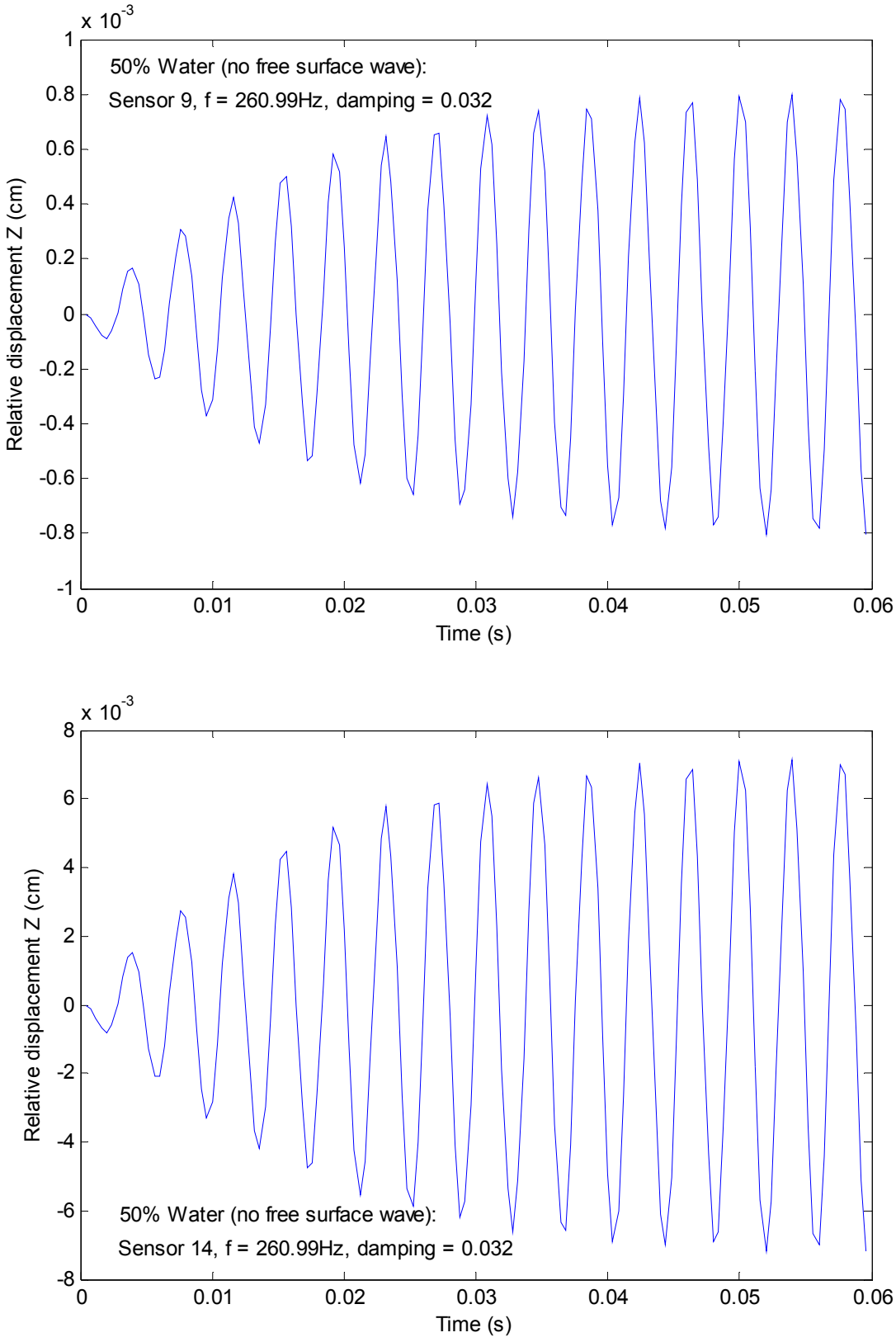

Fig. 4.5 The time response histories in z-direction at top sensor 9 and bottom sensor 14 of the tank

4-4 50% water filled with free surface wave

Base motion

Frequency 1.6248Hz

Acceleration amplitude 1g = 981cm/s^2

Related data in calculation

Retained mode number 10

Maximum frequency of retained modes 3.0848Hz

Damping coefficient 0.032

Time step 0.02s

Calculation time step 300

Output step interval 2

Table 4.4 shows the maximum amplitudes at interest points and arriving times. Fig 4.6 shows the pressure response at points 16a) and 16b). Fig. 4.7 shows the displacement response curves at top sensor point 9 and the bottom sensor point 14. In this case, due to the constant pressure mode with zero frequency, the mean values of the response curves do not equal zero, which is caused by zero frequency motion.

Table 4.4 Maximum displacement and pressure values and arriving time at interest points

Node -(component)	61-(1)	61-(2)	61-(3)	212-(1)	212-(2)	212-(3)
Values (cm)	1.791913D-06	2.448165D-06	3.691236D-04	7.549681D-06	4.763217D-06	3.032478D-04
Time (s)	2.160000D+00	2.160000D+00	9.200000D-01	2.160000D+00	5.840000D+00	9.200000D-01
Node -(component)	252-(1)	252-(2)	252-(3)	292-(1)	292-(2)	292-(3)
Values (cm)	1.481710D-06	3.400669D-06	2.624043D-04	1.569331D-05	1.669615D-05	2.212543D-04
Time (s)	5.840000D+00	9.200000D-01	9.200000D-01	9.200000D-01	9.200000D-01	9.200000D-01
Node -(component)	321-(1)	321-(2)	321-(3)	642-(1)	642-(2)	642-(3)
Values (cm)	1.036716D-05	8.847735D-06	2.373988D-04	1.138359D-05	1.359740D-05	1.469821D-04
Time (s)	9.200000D-01	9.200000D-01	9.200000D-01	4.000000D+00	4.000000D+00	4.000000D+00
Node -(component)	652-(1)	652-(2)	652-(3)	671-(1)	671-(2)	671-(3)
Values (cm)	9.662340D-06	1.321839D-05	1.507026D-04	7.220443D-07	5.032217D-06	1.844108D-04
Time (s)	4.000000D+00	4.000000D+00	4.000000D+00	3.200000D-01	9.200000D-01	4.000000D+00
Node -(component)	681-(1)	681-(2)	681-(3)	836-(1)	836-(2)	836-(3)
Values (cm)	4.097802D-06	6.642083D-06	1.911852D-04	9.103065D-08	9.083971D-06	2.406413D-04
Time (s)	2.160000D+00	2.160000D+00	4.000000D+00	1.520000D+00	4.000000D+00	4.000000D+00
Node -(component)	871-(7)	1022-(7)	1062-(7)	1102-(7)	1131-(7)	
Values (kg/cm2	2.059507D-02	2.059796D-02	2.059990D-02	2.060172D-02	2.060162D-02	
Time (s)	4.000000D+00	4.000000D+00	4.000000D+00	4.000000D+00	4.000000D+00	

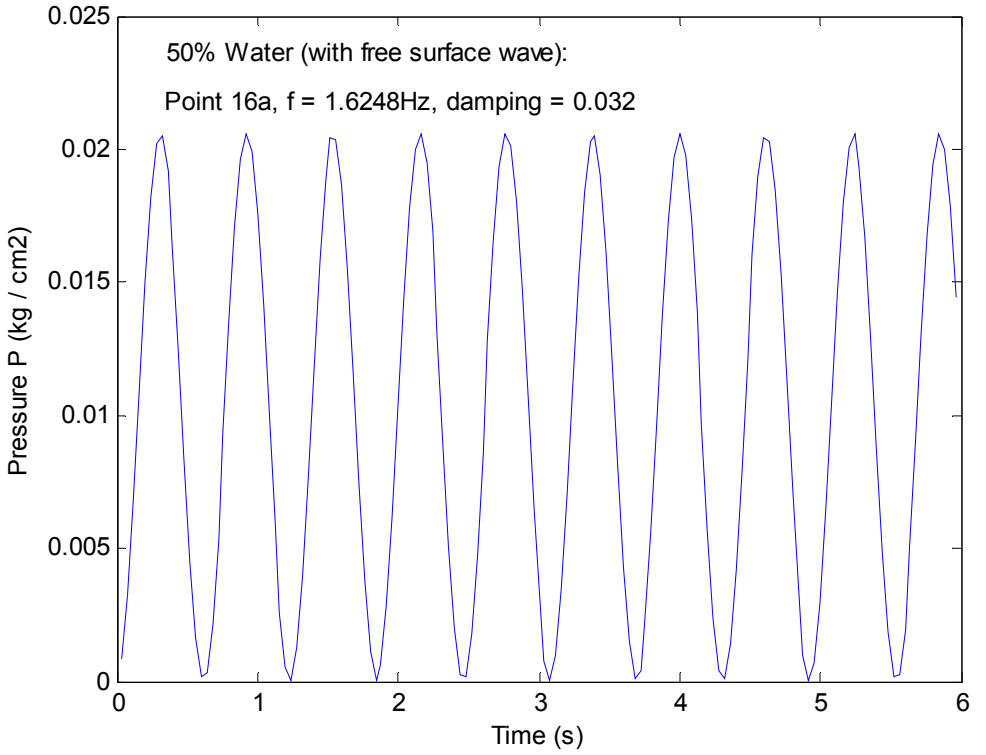

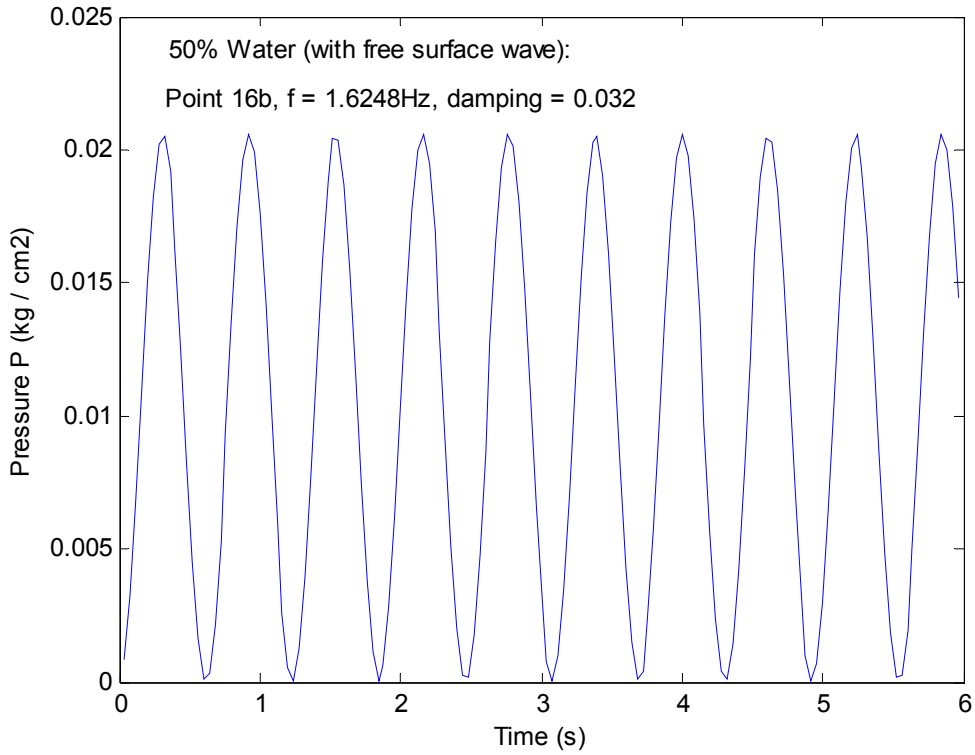

Fig. 4.6 The time response histories at point 16a) and 16b).

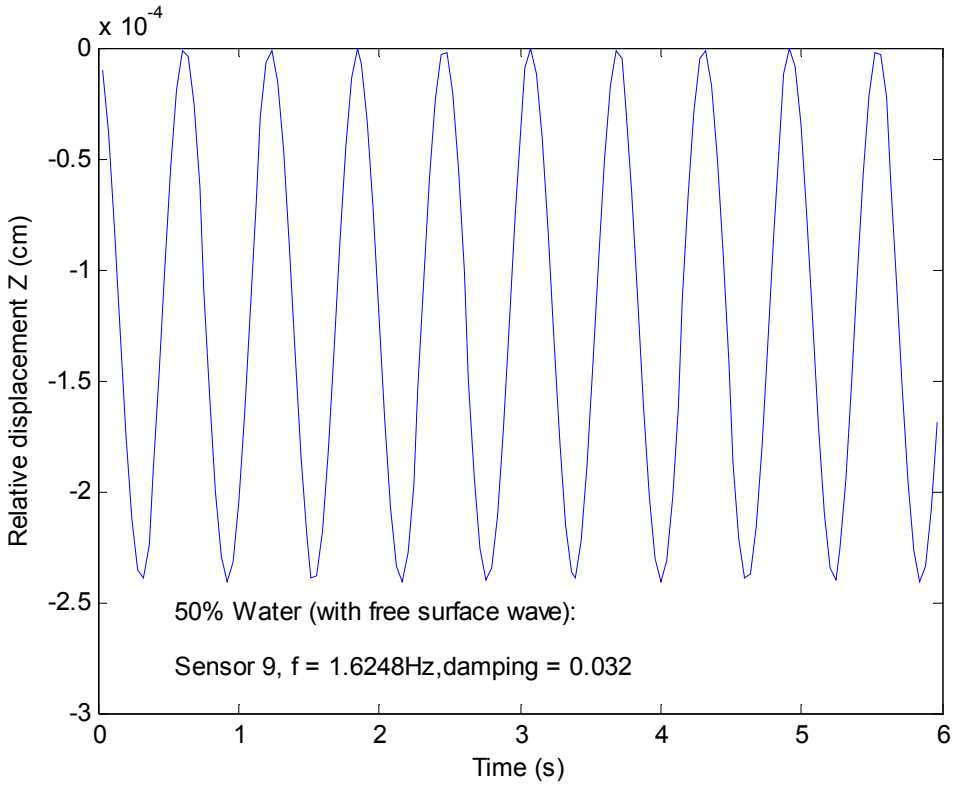

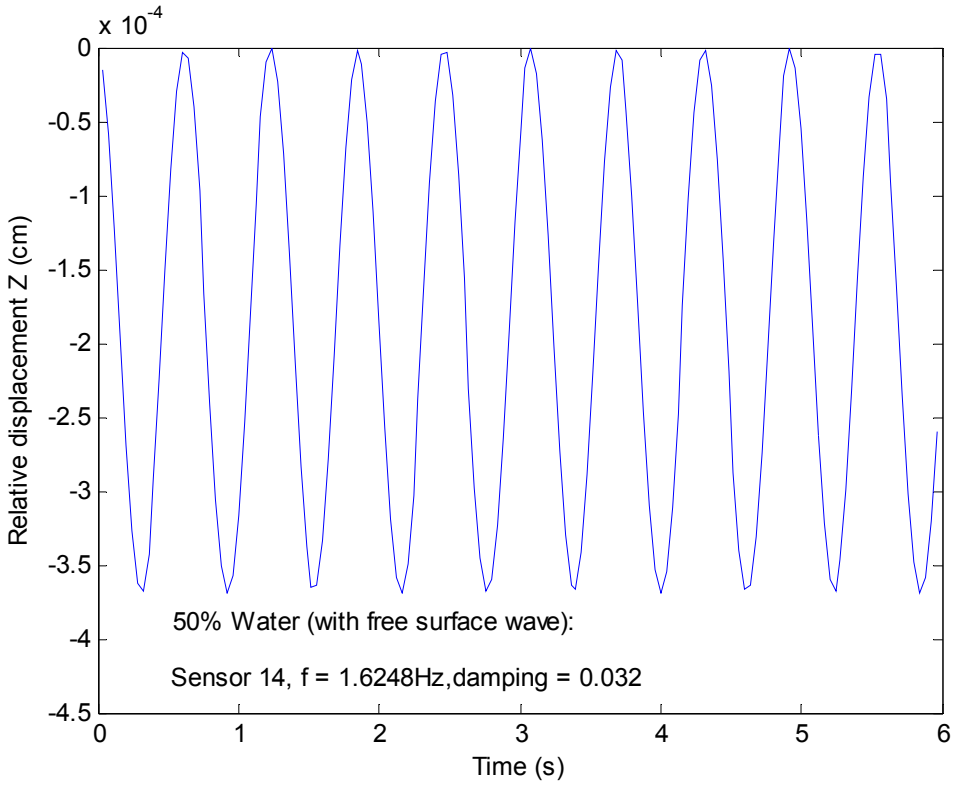

Fig. 4.5 The time response histories in z-direction at top sensor 9 and bottom sensor 14 of the tank

4-5 66% water filled

Base motion

Frequency 252.28Hz

Acceleration amplitude 1g = 981cm/s^2

Related data in calculation

Retained mode number 10

Maximum frequency of retained modes 559.65Hz

Damping coefficient 0.029

Time step 0.0001s

Calculation time step 600

Output step interval 2

Table 4.5 shows the maximum amplitudes at interest points and arriving times. Fig 4.8 shows the pressure response at points 16a) and 16b). Fig. 4.9 shows the displacement response curves at top sensor point 9 and the bottom sensor point 14.

Table 4.5 Maximum displacement and pressure values and arriving time at interest points

Node-(component)	61-(1)	61-(2)	61-(3)	212-(1)	212-(2)	212-(3)
Values (cm)	8.768980D-05	6.951119D-05	1.023628D-02	1.165726D-04	2.320893D-04	8.114638D-03
Time (s)	5.920000D-02	5.940000D-02	5.960000D-02	5.380000D-02	5.940000D-02	5.960000D-02
Node-(component)	252-(1)	252-(2)	252-(3)	292-(1)	292-(2)	292-(3)
Values (cm)	1.939302D-04	9.354674D-05	6.749711D-03	6.606171D-04	5.910388D-04	5.377725D-03
Time (s)	5.940000D-02	5.780000D-02	5.960000D-02	5.960000D-02	5.960000D-02	5.960000D-02
Node-(component)	321-(1)	321-(2)	321-(3)	682-(1)	682-(2)	682-(3)
Values (cm)	6.470878D-04	6.323637D-04	5.421656D-03	4.012245D-05	3.893212D-05	1.446944D-03
Time (s)	5.940000D-02	5.960000D-02	5.960000D-02	5.960000D-02	5.960000D-02	5.960000D-02
Node-(component)	692-(1)	692-(2)	692-(3)	711-(1)	711-(2)	711-(3)
Values (cm)	1.116211D-05	2.757910D-05	1.370498D-03	3.399894D-05	1.243302D-05	1.376155D-03
Time (s)	1.400000D-03	5.600000D-02	5.960000D-02	5.600000D-02	5.960000D-02	5.960000D-02
Node-(component)	721-(1)	721-(2)	721-(3)	876-(1)	876-(2)	876-(3)
Values (cm)	5.631006D-05	5.095552D-05	1.393772D-03	2.368695D-05	2.596985D-05	1.375100D-03
Time (s)	5.940000D-02	5.960000D-02	5.960000D-02	5.940000D-02	5.940000D-02	5.960000D-02
Node-(component)	1033-(7)	1184-(7)	1224-(7)	1264-(7)	1293-(7)	
Values (kg/cm2	3.409952D-01	2.609487D-01	2.119302D-01	1.610124D-01	1.601019D-01	
Time (s)	5.960000D-02	5.960000D-02	5.960000D-02	5.960000D-02	5.960000D-02	

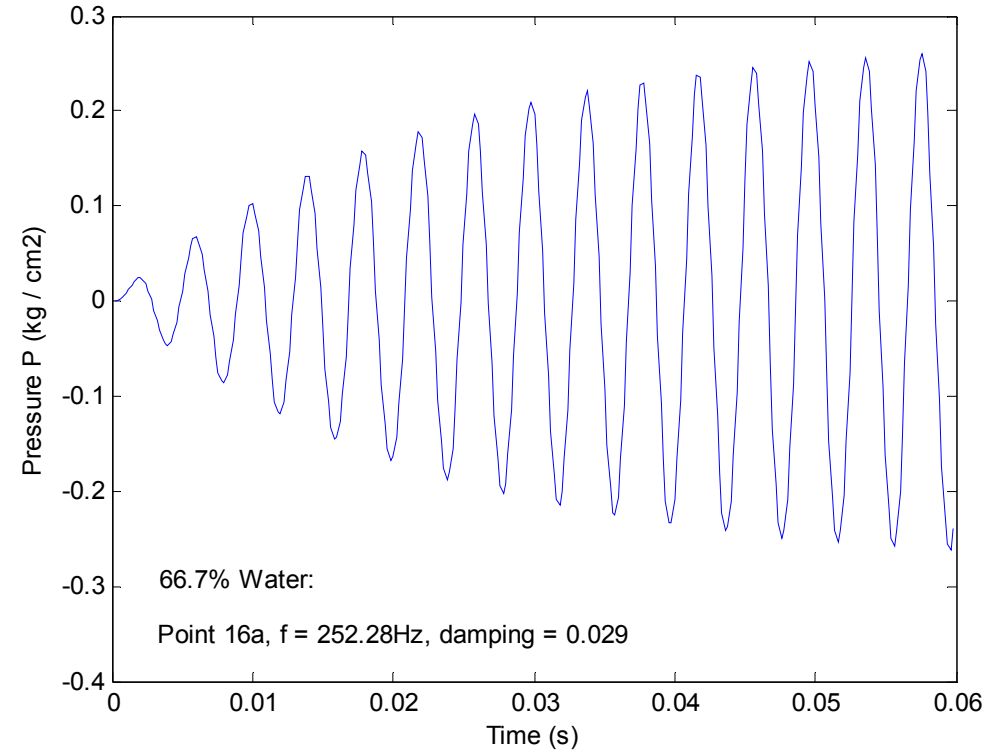

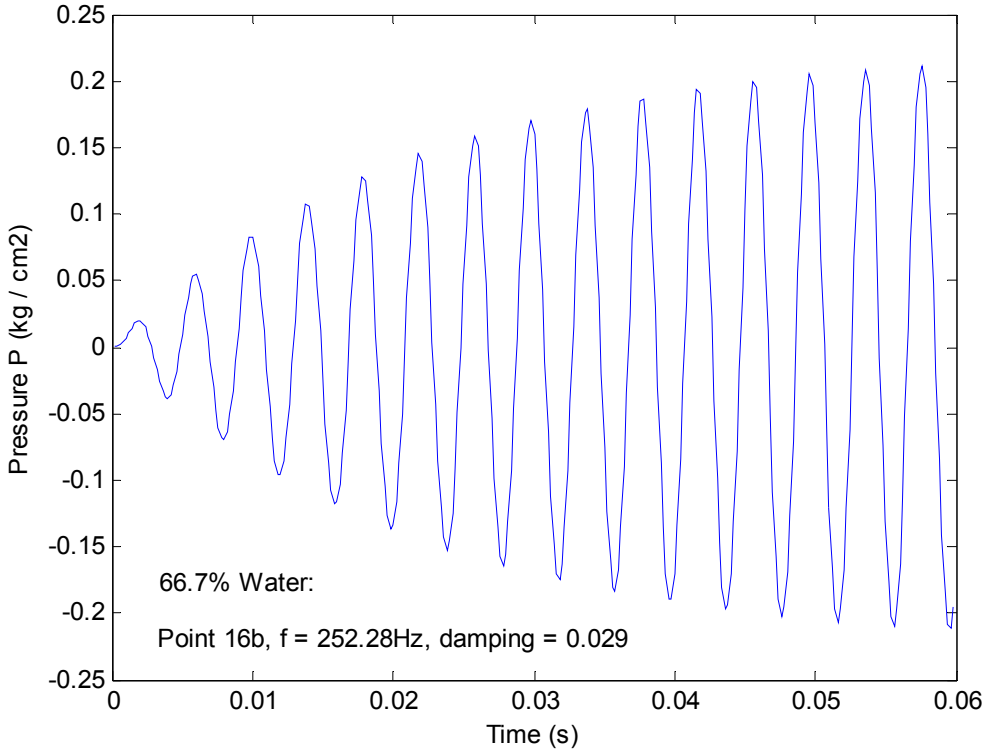

Fig. 4.8 The time response histories at point 16a) and 16b).

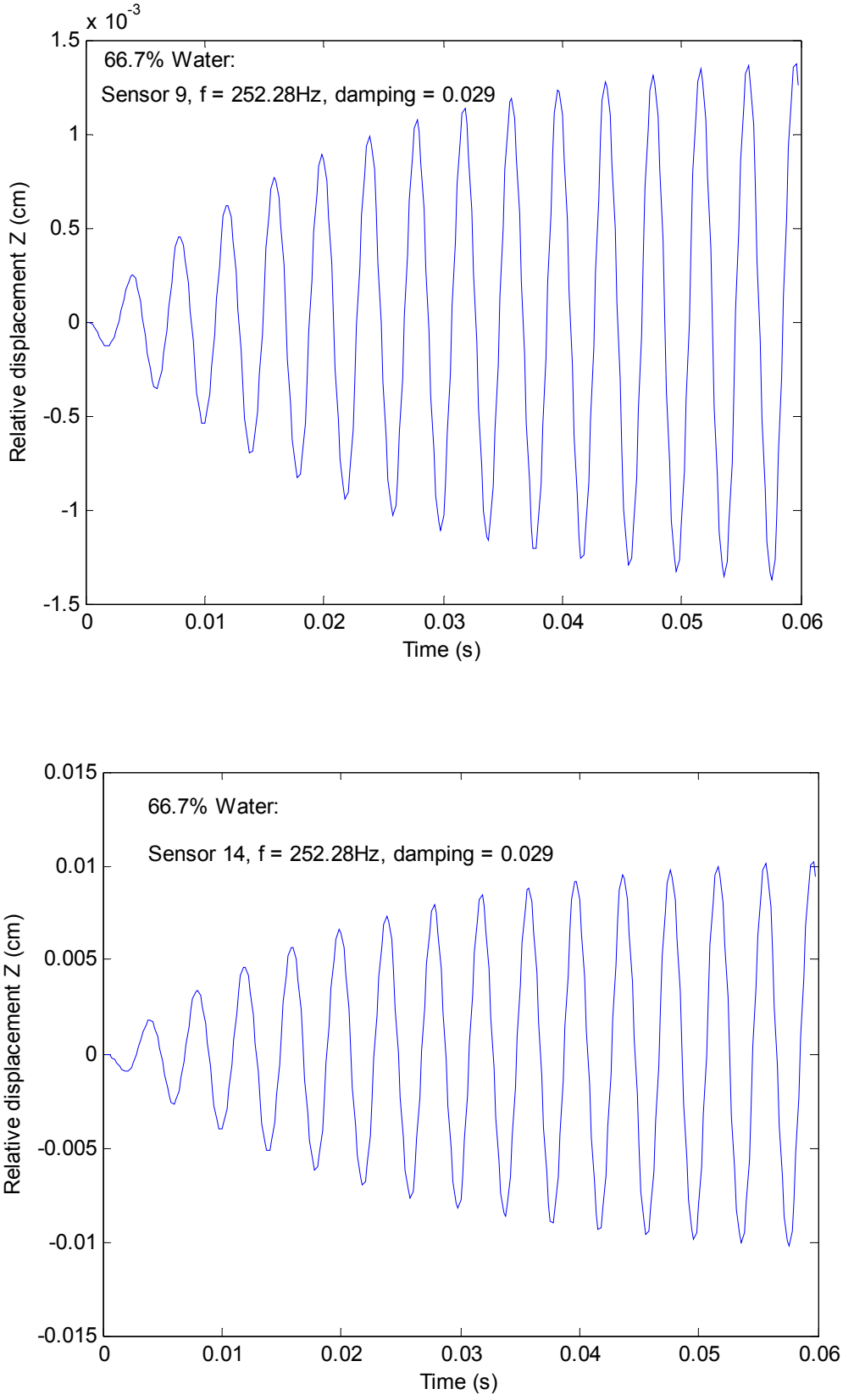

Fig. 4.9 The time response histories in z-direction at top sensor 9 and bottom sensor 14 of the tank

4-6 Fully filled tank

Base motion

Frequency 201.24Hz

Acceleration amplitude 1g = 981cm/s^2

Related data in calculation

Retained mode number 10

Maximum frequency of retained modes 453.71Hz

Damping coefficient 0.031

Time step 0.0002s

Calculation time step 300

Output step interval 2

Table 4.6 shows the maximum amplitudes at interest points and arriving times. Fig 4.10 shows the pressure response at points 15, 16a) and 16b). Fig. 4.11 shows the displacement response curves at top sensor point 9 and the bottom sensor point 14.

Table 4.6 Maximum displacement and pressure values and arriving time at interest points

Node -(component)	61-(1)	61-(2)	61-(3)	212-(1)	212-(2)	212-(3)
Values (cm)	6.525720D-05	5.217052D-05	1.249957D-02	2.330684D-04	2.721218D-04	1.038725D-02
Time (s)	5.880000D-02	5.920000D-02	5.480000D-02	5.760000D-02	5.720000D-02	5.480000D-02
Node -(component)	252-(1)	252-(2)	252-(3)	292-(1)	292-(2)	292-(3)
Values (cm)	8.754442D-05	4.147590D-05	9.017926D-03	5.389028D-04	4.885109D-04	7.632590D-03
Time (s)	5.920000D-02	5.560000D-02	5.480000D-02	5.720000D-02	5.240000D-02	5.480000D-02
Node -(component)	321-(1)	321-(2)	321-(3)	642-(1)	642-(2)	642-(3)
Values (cm)	5.087057D-04	5.026793D-04	7.649083D-03	3.795461D-04	3.644999D-04	5.744757D-03
Time (s)	5.720000D-02	5.720000D-02	5.480000D-02	5.720000D-02	5.720000D-02	5.480000D-02
Node -(component)	652-(1)	652-(2)	652-(3)	671-(1)	671-(2)	671-(3)
Values (cm)	1.978298D-04	3.001390D-04	5.885756D-03	2.949310D-04	1.628990D-04	5.986549D-03
Time (s)	5.240000D-02	5.720000D-02	5.480000D-02	5.720000D-02	5.480000D-02	5.480000D-02
Node -(component)	681-(1)	681-(2)	681-(3)	836-(1)	836-(2)	836-(3)
Values (cm)	1.271819D-04	1.248090D-04	6.116592D-03	8.676367D-05	2.175266D-04	9.040959D-03
Time (s)	5.000000D-02	5.240000D-02	5.480000D-02	5.960000D-02	5.720000D-02	5.480000D-02
Node -(component)	1519-(7)	1670-(7)	1710-(7)	1750-(7)	1779-(7)	2100-(7)
Values(kg/cm2)	8.226359D-01	7.630379D-01	7.257821D-01	6.863414D-01	6.862409D-01	4.613993D-01
Time (s)	5.480000D-02	5.480000D-02	5.480000D-02	5.480000D-02	5.480000D-02	5.480000D-02

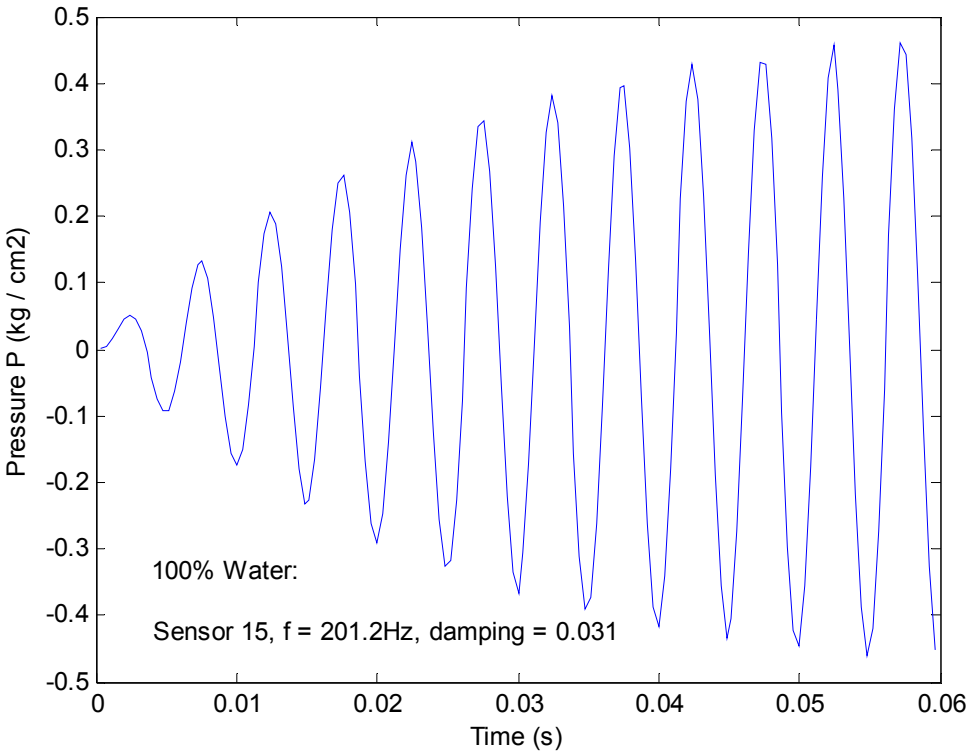
0.5
0.4
0.3
0.2
0.1
0
-0.1
-0.2
-0.3
-0.4
-0.5
Pressure P (kg / cm2)
100% Water:
Sensor 15, f = 201.2Hz, damping = 0.031
0
0.01
0.02
0.03
0.04
0.05
0.06
Time (s)

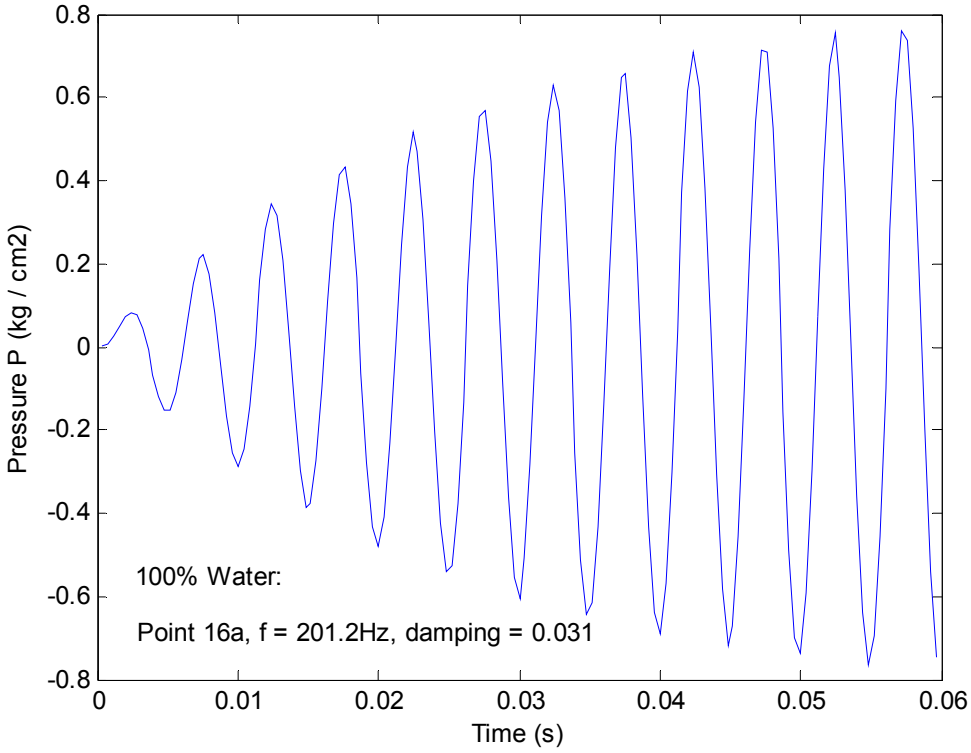
0.8
0.6
0.4
0.2
0
-0.2
-0.4
-0.6
-0.8
Pressure P (kg / cm2)
100% Water:
Point 16a, f = 201.2Hz, damping = 0.031
0
0.01
0.02
0.03
0.04
0.05
0.06
Time (s)

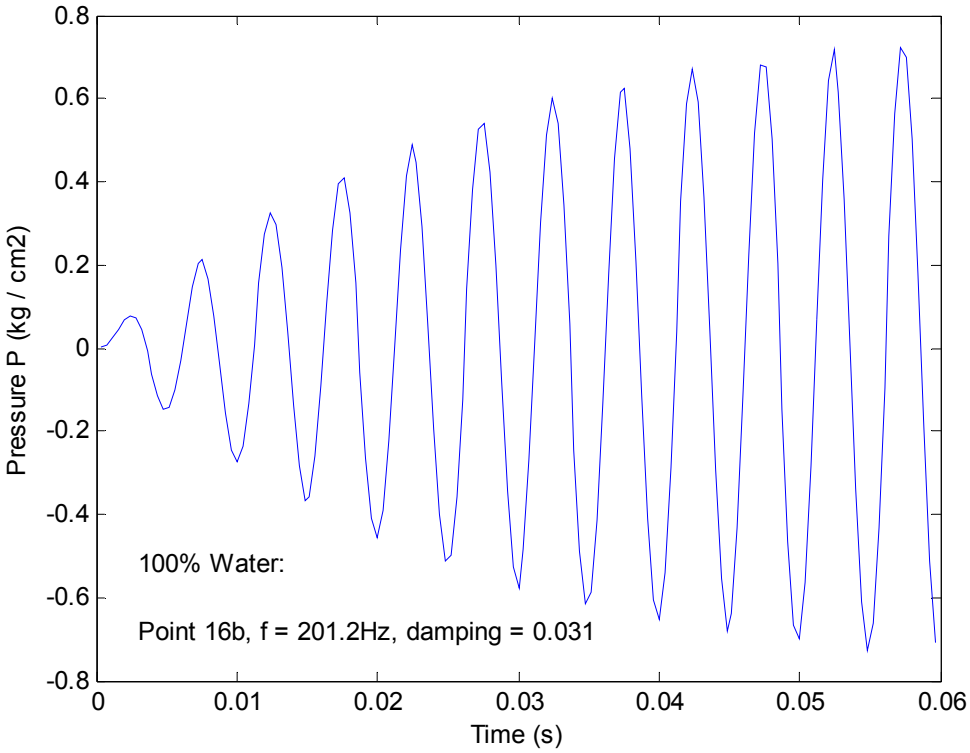

Fig 4.10 shows the pressure response at points 15, 16a) and 16b)

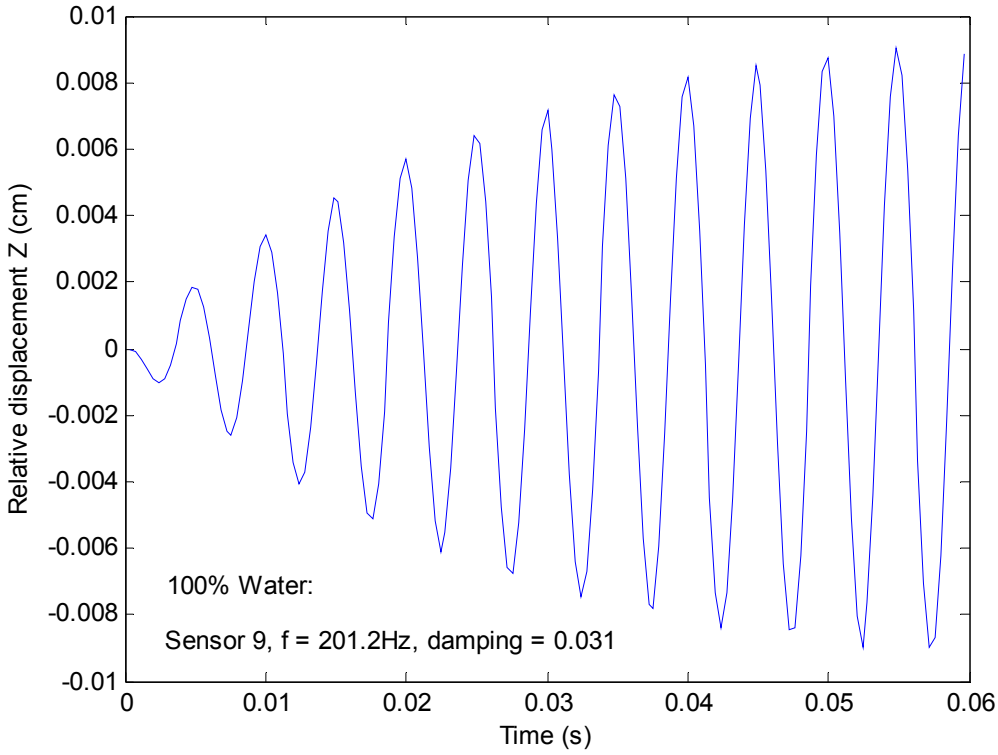

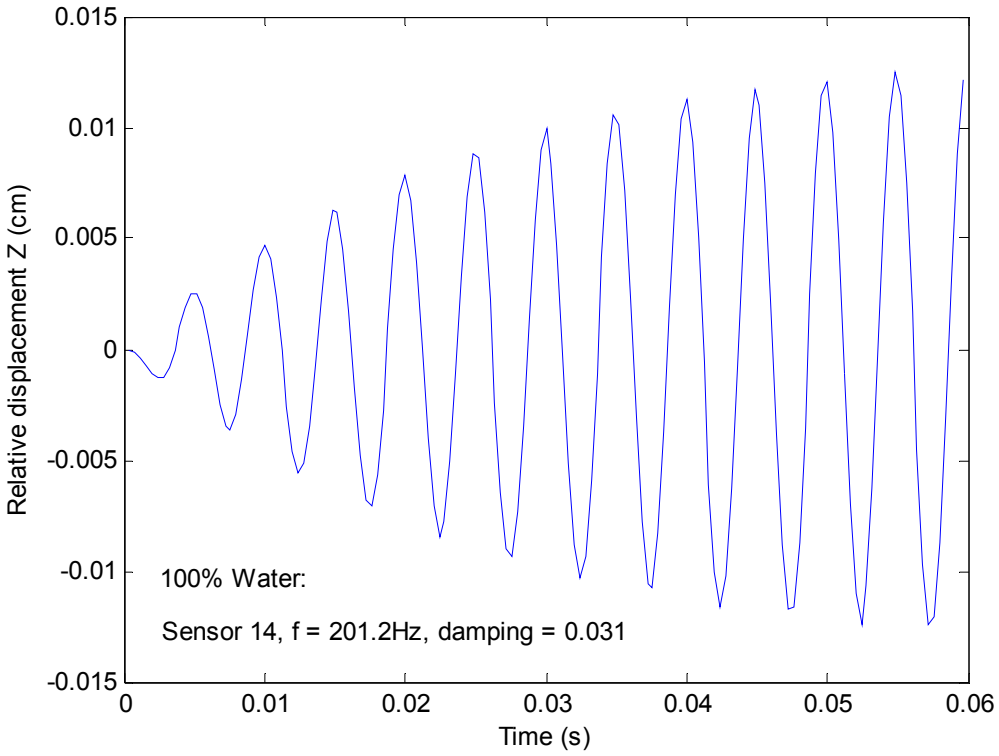

Fig. 4.11 shows the displacement response curves at top sensor point 9 and bottom sensor point 14.

4-7 Discussion and explanation

The dynamic response of the water-tank system is affected by the mode damping coefficients. The values of these coefficients are approximately provided only for one mode. Following the rule of mode reduction, the modes of frequencies lower than about 2.0 – 3.0 times of excitation frequency are retained to conduct the response analysis. For each retained mode, the damping coefficient practically is different each other. In calculations, we use a same damping for all modes retained to conduct the analysis of each case. Therefore, the response analysis results are for reference.

Theoretically, the dynamic response solution consists of a free vibration and a forced vibration. For the system with no free surface wave considered, there is no zero frequency modes in the system and the free vibration components are decreased with the time going due to the damping effect. However, for the case of free surface wave considered, there is a zero constant pressure mode for which the initial displacement and pressure or the velocity does not affected by damping. As result of this, the mean values of the response curves are constants. For dynamic strength design, the suggestion is to use the maximum amplitude that is the amplitude of the stable forced response, to conduct the analysis. The maximum amplitudes and their arriving times are given in the data files. For the case of free surface wave considered, the mean value should be subtracted from the given maximum value.

It is suggested that the sloshing modes should be included if the system is operated in a vibration environment with the lower frequencies of excitation force or base motion. For the vibration environment with only higher frequencies excitations, the free surface wave can be neglected.

Conclusions

This joint research project clarifies and confirms the following points:

1) Due to water – tank interaction, the natural frequencies of the water – tank system are decreased with the water level increase. For the 25% water level, the natural frequencies, especially heave mode frequency, shows a significant decrease compared with the empty case. However, with continuing increase the filed water more than 25% level, the decrease gradient of the natural frequencies gradually tends to zero. In the 100% water case, the natural frequency of heave mode is about 200 Hz which can not equal zero.
2) Considering free surface wave effect produces a lot of sloshing modes of very low frequencies compared with the natural frequencies of the dry tank structure. Therefore, for dynamic response analysis with high frequency excitations, the free surface wave may be neglected. However, to assess loads caused by sloshing modes, the free surface waves have to be considered.
3) There exist relative big deformations at the four tank support places in several vibration modes, which may produce a large local stress at support places to cause the product fail in vibration environment. A strengthen local design at the support places is needed.
4) The dynamic response results are affected by damping coefficients of all modes used in the dynamic response analysis. The damping coefficients are approximately presented and therefore, the numerical results are good reference for practical designs.

The report confirms that the original purpose of this joint research project has well completed by IHI and SES.

Appendices

For each studied case, an input file and output file are provided in the disk. These files provide all information used in the calculations and the results obtained. The 20 data files and explanations are as follows.

0%freq-in input file for natural frequency calculation of 0% water filed tank
0%freq-out output file for natural frequency calculation of 0% water filed tank
0%resp-in input file for dynamic response calculation of 0% water filed tank
0%resp-out output file for dynamic response calculation of 0% water filed tank

50%freq-in input file for natural frequency calculation of 50% water filed tank
50%freq-out output file for natural frequency calculation of 50% water filed tank
50%resp-in input file for dynamic response calculation of 50% water filed tank
50%resp-out output file for dynamic response calculation of 50% water filed tank

50%freq-sw-in input file for natural frequency calculation of 50% water tank + surface wave
50%freq-sw-out output file for natural frequency calculation of 50% water tank+ surface wave
50%resp-sw-in input file for dynamic response calculation of 50% water tank+ surface wave
50%resp-sw-out output file for dynamic response calculation of 50% water tank+ surface wave

66%freq-in input file for natural frequency calculation of 66% water filed tank
66%freq-out output file for natural frequency calculation of 66% water filed tank
66%resp-in input file for dynamic response calculation of 66% water filed tank
66%resp-out output file for dynamic response calculation of 66% water filed tank

100%freq-in input file for natural frequency calculation of 100% water filed tank
100%freq-out output file for natural frequency calculation of 100% water filed tank
100%resp-in input file for dynamic response calculation of 100% water filed tank
100%resp-out output file for dynamic response calculation of 100% water filed tank

References

Bathe, K.J. (1996) *Finite element procedures*, New Jersey: Prentice Hall.

Fung Y.C. *A First Course in Continuum Mechanics.* Prentice-Hall, 1977.

Xing, J.T. & Price, W.G. (1991). A mixed finite element method for the dynamic analysis of coupled fluid-solid interaction problems. *Proc. R. Soc. Lond. A***433**, pp235-255.

Xing J.T. (1995a). *Theoretical manual of fluid-structure interaction analysis program-FSIAP*, School of Engineering Sciences, University of Southampton.

Xing J.T. (1995b) *User manual fluid-structure interaction analysis program-FSIAP*, School of Engineering Sciences, University of Southampton.

Xing J.T., Price, W.G. & Du, Q.H. (1996). Mixed finite element substructure-subdomain methods for the dynamical analysis of coupled fluid-solid interaction problems. *Phil. Trans. R. S. Lond.* A **354**, pp259-295.

Xing, J.T., Price, W.G. & Wang, A. (1997). Transient analysis of the ship-water interaction system excited by a pressure water wave, *Marine Structures,* **10**(5), pp305-321.

Zienkiewicz, O.C. and Taylor, R.L. (1989/1991) *The finite element method,* 4th edn, Vol 1 (1989), Vol 2 (1991). New York: McGraw-Hill